Journal of Medicinal Chemistry

Article

pubs.acs.org/jmc

Synthesis and Evaluation of Indole-Based Chalcones as Inducers of Methuosis, a Novel Type of Nonapoptotic Cell Death

Michael W. Robinson,[†,‡] Jean H. Overmeyer,[†] Ashley M. Young,[†] Paul W. Erhardt,*[,‡] and William A. Maltese*[,†]

[†]Department of Biochemistry and Cancer Biology, University of Toledo College of Medicine, 3000 Arlington Ave., Toledo, Ohio 43614, United States

[‡]Center for Drug Design and Development, Department of Medicinal and Biological Chemistry, University of Toledo College of Pharmacy, 2801 W. Bancroft Ave., Toledo, Ohio 43606, United States

Supporting Information

ABSTRACT: Methuosis is a novel caspase-independent form of cell death in which massive accumulation of vacuoles derived from macropinosomes ultimately causes cells to detach from the substratum and rupture. We recently described a chalcone-like compound, 3-(2-methyl-1*H*-indol-3-yl)-1-(4-pyridinyl)-2-propen-1-one (i.e., MIPP), which can induce methuosis in glioblastoma and other types of cancer cells. Herein, we describe the synthesis and structure−activity relationships of a directed library of related compounds, providing insights into the contributions of the two aryl ring systems and highlighting a potent derivative, 3-(5-methoxy, 2-methyl-1*H*-indol-3-yl)-1-(4-pyridinyl)-2-propen-1-one (i.e., MOMIPP) that can induce methuosis at low micromolar concentrations. We have also generated biologically active azide derivatives that may be useful for future studies aimed at identifying the protein targets of MOMIPP by photoaffinity labeling techniques. The potential significance of these studies is underscored by the finding that MOMIPP effectively reduces the growth and viability of Temozolomide-resistant glioblastoma and doxorubicin-resistant breast cancer cells. Thus, it may serve as a prototype for drugs that could be used to trigger death by methuosis in cancers that are resistant to conventional forms of cell death (e.g., apoptosis).

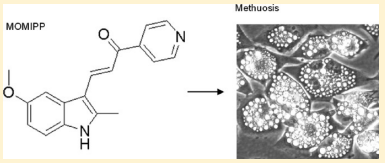

INTRODUCTION

Despite recent advances in developing therapeutic agents that target regulatory pathways unique to certain types of cancer cells, the mainstays for postsurgical adjuvant therapy of many tumors remain radiation and DNA alkylating agents. An example is the highly malignant brain tumor, glioblastoma multiforme (GBM), where the current standard of care involves surgery when possible, followed by adjuvant therapy with radiation and oral Temozolomide (TMZ).[1] A limitation of the latter approaches is that they work by damaging DNA, triggering the intrinsic apoptotic pathway.[2] Because GBM cells typically harbor mutations in tumor suppressor genes (e.g., PTEN, p53, and pRB), they are relatively insensitive to apoptotic stimuli.[3,4] Moreover, glioblastoma cells develop resistance to alkylating agents by increasing their capacity to repair DNA lesions.[5] We believe that it may be possible to develop new approaches to treat such drug-resistant cancers through the induction of alternative nonapoptotic forms of cell death, which do not depend on DNA damage as a trigger. Toward this end, we have defined a unique form of cell death termed "methuosis".[6,7]

The hallmark of methuosis is the displacement of much of the cellular cytoplasmic space by vacuoles derived from macropinosomes.[6] The latter are formed when membrane ruffles (lamellipodia) enclose pockets of extracellular fluid and are internalized.[8,9] In methuosis, impairment of the recycling and lysosome-directed trafficking of macropinocytotic vesicles locks them in an intermediate stage where they fuse to form progressively larger vacuoles. This eventually causes a decrease in metabolic activity and rupture of the cell membrane.[6] Death is considered to be nonapoptotic, as is it is not accompanied by nuclear chromatin condensation, cell blebbing, or nucleosomal DNA fragmentation. Methuosis is also caspase-independent, as it cannot be prevented by broad-spectrum caspase inhibitors such as zVAD-fmk.[6]

Methuosis was initially characterized in GBM cells, where this form of cell death was triggered by ectopic expression of activated Ras and Rac GTPases. However, the potential for exploiting this nonconventional cell death pathway to kill cancer cells that are refractory to apoptosis depends on the identification of molecules with druglike properties that can induce methuosis. We recently described a prototype chalcone-related compound that can induce cell death with the hallmarks of methuosis in both TMZ-resistant and nonresistant GBM cells, as well as other cancer cell lines derived from breast, colon, and pancreas.[10] Herein, we report synthesis and structure−activity relationship (SAR) studies of a directed library of related compounds leading to (1) the definition of key features required for methuosis-inducing activity, (2) the identification of a derivative with improved biological activity, and (3) the development of an active azide analogue that may be suitable for use as a photoaffinity probe in future target identification efforts.

Received: July 27, 2011
Published: February 15, 2012

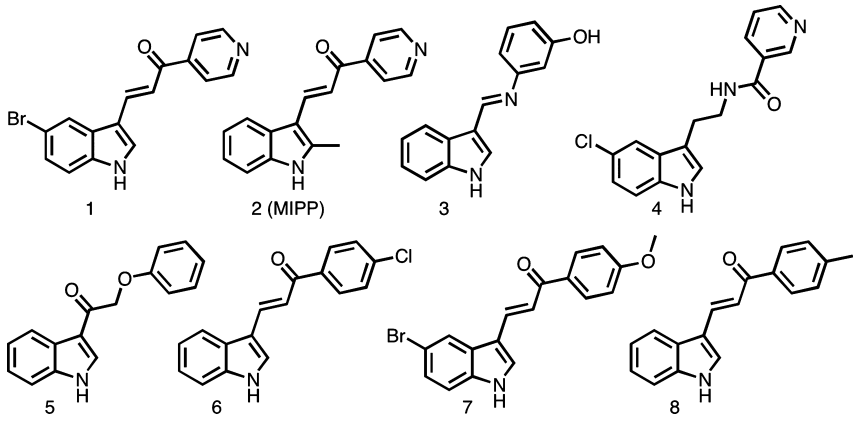

Figure 1. Structures of compounds **1** and **2**, initially found to be active inducers of methuosis[10] as compared with commercially available analogues **3**–**8**, which failed to induce the hallmarks of methuosis in culture U251 GBM cells.

Scheme 1. Synthesis of Analogues of MIPP (Compound 2)[a]

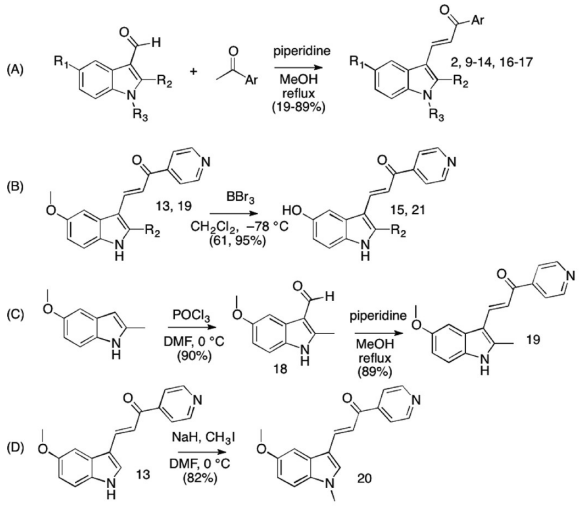

cmpd #	R_1	R_2	R_3	Ar
2 (MIPP)	H	CH_3	H	
9	H	H	H	
10	H	H	H	
11	H	H	H	
12	H	H	H	
13	CH_3O	H	H	
14		H	H	
15	OH	H	H	
16	CH_3O	H	H	
17	CH_3O	H	H	
19 (MOMIPP)	CH_3O	CH_3	H	
20	CH_3O	H	CH_3	
21	OH	CH_3	H	

[a]The specific substituents at R_1, R_2, R_3, and Ar for each numbered compound are listed in the chart. For A–D, the specific conditions and reagents were as follows: (A) piperidine, CH_3OH, reflux, 19–89%. (B) BBr_3, CH_2Cl_2, −78 °C, 61 and 95% for **15** and **21**, respectively. (C) $POCl_3$, DMF, 0 °C, 90%; piperidine, CH_3OH, reflux, 89%. (D) NaH, CH_3I, DMF, RT, 82%.

RESULTS

SARs. As we began to seek druglike small molecules that could trigger methuosis, we noted a report from Kirchhausen and colleagues[11] in which they described a molecule termed vacuolin-1, along with several other triazine-based compounds, that were capable of inhibiting Ca^{2+}-dependent lysosomal exocytosis. Although these compounds induced marked cellular vacuolization, they did not cause cell death. However, in the Supporting Information included with this report, a structurally distinct vacuole-inducing compound captured our attention because of its resemblance to a class of molecules termed chalcones. The structure of this compound is depicted in Figure 1 (compound **1**). Chalcones consist of a 1,3-diphenyl-2-propen-1-one framework that serves as a precursor for flavonoid natural products. However, the term chalcones has been applied more broadly to describe a number of synthetic derivatives built on this framework.[12] Several chalcones have been found to have significant anticancer activity but have not been reported to induce vacuolization of cells.[12−14] This prompted us to ask whether compound **1** might represent a novel type of chalcone that can kill cancer cells by inducing methuosis. We found that compound **1** caused extensive vacuolization of glioblastoma cells within a few hours and substantial loss of cell viability within 48 h.[10] Chemical database searches yielded additional compounds with >75% similarity to **1**. Among these, compound **2** (Figure 1) was selected for further study. It induced vacuoles that were larger and more numerous than those produced by compound **1**. Compound **2** was assigned the acronym MIPP, that is, 3-(2-methyl-1*H*-indol-3-yl)-1-(4-pyridinyl)-2-propen-1-one. Detailed evaluation of the biological effects of MIPP indicated that the form of cell death induced by this compound matched the profile of methuosis.[10] Furthermore, MIPP was effective in reducing the growth and viability of GBM cells that were highly resistant to TMZ.[10]

Because concentrations of MIPP ≥ 10 μM were required to effectively induce methuosis, we began to assemble a directed library of MIPP-related compounds and conducted initial SAR comparisons with the goal of identifying analogues with improved potency. We began by comparing the methuosis-inducing activity of MIPP with several closely related compounds that were commercially available (compounds **3**–**8** in Figure 1). The latter did not trigger cellular vacuolization when added to U251 GBM cells at a concentration of 10 μM. Examination of compounds **1**–**8** (Figure 1) suggested that the

dx.doi.org/10.1021/jm201006x | *J. Med. Chem.* 2012, 55, 1940–1956

Table 1. Summary of SAR Studies Performed on MIPP (Compound 2) and Related Compounds Generated in Schemes 1 and 2

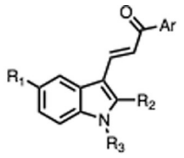

cmpd #	R_1	R_2	R_3	Ar	Viability (MTT*)	Colony Formation*	Vacuoles?
2 (MIPP)	H	CH_3	H		24 ± 3	8 ± 4	yes
9	H	H	H		109 ± 7	76 ± 7	no
10	H	H	H		96 ± 9	53 ± 10	no
11	H	H	H		72 ± 6	71 ± 10	no
12	H	H	H		58 ± 7	22 ± 2	yes
13	CH_3O	H	H		58 ± 2	2 ± 1	yes
14		H	H		56 ± 4	8 ± 2	yes
15	OH	H	H		107 ± 22	72 ± 6	no
16	CH_3O	H	H		90 ± 8	99 ± 30	no
17	CH_3O	H	H		88 ± 8	96 ± 22	no
19 (MOMIPP)	CH_3O	CH_3	H		12 ± 2	0	yes
20	CH_3O	H	CH_3		73 ± 13	52 ± 9	yes
21	OH	CH_3	H		101 ± 13	43 ± 17	yes
26	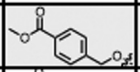	CH_3	H		79 ± 2	76 ± 8	no
27	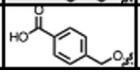	CH_3	H		79 ± 9	71 ± 11	no

*Results are expressed as percent of controls that received vehicle alone (DMSO). Values are the mean ± SD of quadruplicate (MTT) or triplicate (colony formation) determinations.

specific relationship between an indole and a pyridinyl ring was likely to be playing a significant role in determining activity. Specifically, comparison of compound **1** (active) with compound **7** (inactive) demonstrated the importance of the pyridinyl ring, because replacement of the latter with a *para*-methoxy phenyl ring rendered the compound inactive. Therefore, an initial set of analogues was synthesized to investigate the influence of the position of the pyridine nitrogen on biological activity.

Analogues based on the α,β-unsaturated ketone core can be prepared by Claisen−Schmidt condensations between indole-3-carboxaldehydes and aryl ketones.[15] Condensation of acetophenone or various acetyl-pyridines with indole-3-carboxaldehyde yielded compounds **9**−**12** (Scheme 1A). The activities of these compounds were compared to MIPP at a concentration of 10 μM using three criteria: (1) morphological vacuolization of live cells assessed by phase contrast microscopy at 24 and 48 h; (2) cell viability at a 48 h end point assessed by 3-(4,5-dimethylthiazol-2-yl)-2,5-diphenyl tetrazolium bromide (MTT) assay, with fresh compound added after the first 24 h; and (3) colony-forming assays (2 week end point) performed on cells exposed to the compounds for 48 h. The results of this analysis (Table 1) indicated that a *para*-nitrogen orientation of the pyridine ring is a key feature required for activity. The *meta* and *ortho* analogues **10** and **11**, as well as the acetophenone analogue **9**, were all relatively ineffective at inducing methuosis as compared to MIPP. In contrast, removal of the 2-methyl from the indole ring of MIPP (compound **12**) reduced but did not eliminate activity.

We next explored the consequences of functionalizing the 5-position of the indole ring using commercially available 5-methoxy and 5-benzyloxy indole-3-carboxaldehydes to prepare compounds **13** and **14**, respectively. The 5-methoxy compound **13**, in turn, was demethylated with BBr_3 to afford the 5-OH compound **15** (Scheme 1B). As shown in Table 1, the activities of compounds **13** and **14** were similar to MIPP when compared

dx.doi.org/10.1021/jm201006x | J. Med. Chem. 2012, 55, 1940−1956

Scheme 2. Analogues with 5′ Modifications of the Indole Ring Generated by Functionalizing the Indole Prior to Introduction of the Pyridine Moiety[a]

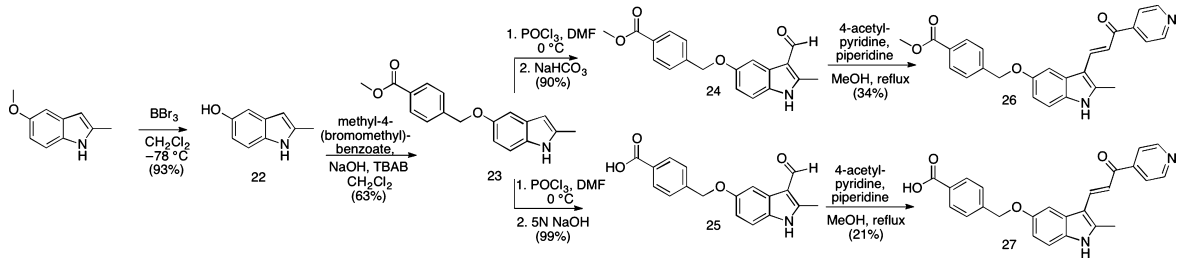

[a]Conditions and reagents: Compound **22**: BBr_3, CH_2Cl_2, −78 °C, 93%. Compound **23**: methyl-4-(bromomethyl)benzoate, NaOH, TBAB, CH_2Cl_2, RT, 63%. Compound **24**: (1) $POCl_3$, DMF, 0 °C; (2) $NaHCO_3$, 90%. Compound **25**: (1) $POCl_3$, DMF, 0 °C; (2) 5 N NaOH, 99%. Compound **26**: 4-acetyl-pyridine, piperidine, MeOH, reflux, 34%. Compound **27**: 4-acetyl-pyridine, piperidine, MeOH, reflux, 21%.

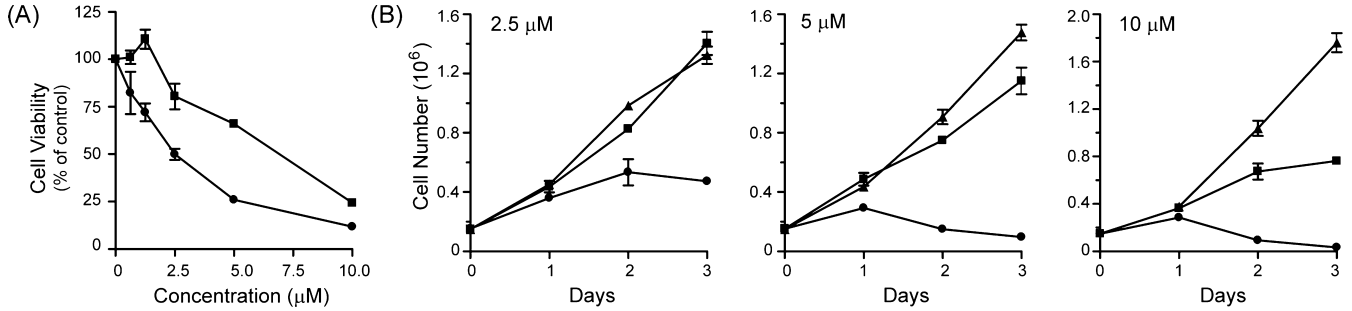

Figure 2. Comparison of the effects of MOMIPP (compound **19**) and MIPP (compound **2**) on growth and viability of U251 GBM cells. (A). One day after plating the cells in 96-well dishes, MOMIPP (●) or MIPP (■) was added at the indicated concentrations. Controls consisted of cells in parallel wells treated with an equivalent volume of vehicle (DMSO). Medium containing fresh compound was added after 24 h, and MTT assays were performed after a total 48 h of treatment. Each point represents the mean (±SD) from four separate wells, with the results expressed as percent of the mean of the parallel control wells. (B) U251 cells seeded in parallel 35 mm dishes were treated with MOMIPP (●), MIPP (■), or an equivalent volume of DMSO (▲), and cells were harvested for counting on each of three consecutive days. Each point is a mean ± SD from three separate cultures.

by colony-forming assay and cell morphology, although they were not as cytotoxic in the short-term growth/viability assay. In contrast, the 5-OH substituent, compound **15**, exhibited greatly reduced biological activity in all of the assays. To confirm that the location of the pyridine nitrogen was still crucial for activity of the 5-methoxy-substituted compounds, analogues **16** and **17** were generated. Loss of activity confirmed the necessity of the *para*-nitrogen (Table 1).

Because comparisons of compounds **12**−**15** versus MIPP suggested that modifications at the 5- and 2-positions of the indole ring both affect activity, we generated a 2-methyl-5-methoxy analogue starting from commercially available 2-methyl-5-methoxy-indole. Key intermediate **18** was synthesized by a Vilsmeier−Haack formylation of 2-methyl-5-methoxyindole, followed by coupling with 4-acetyl-pyridine to yield **19** (Scheme 1C). The inhibitory activity of this compound exceeded that of MIPP in both the MTT viability assay and the colony formation assay (Table 1). Alternatively, methylation of the indole-nitrogen of compound **13** with NaH/CH_3I in dimethylformamide (DMF) (Scheme 1D) to yield **20** produced a compound that induced some cytoplasmic vacuolization but had only modest effects on cell viability (Table 1). Thus, after comparing compounds **13**, **19**, and **20**, it became clear that optimal activity is achieved when the 1- and 2-positions of the indole are occupied by H and methyl, respectively. The 5-OH compound **21**, made by BBr_3 demethylation of **19** (Scheme 1B), showed a marked reduction in activity as compared to the 5-methoxy compound **19** (Table 1), consistent with the detrimental effect of the 5-OH previously observed in compound **15**.

One of the limitations for using MIPP under physiological conditions is its sparing solubility in aqueous solutions. Therefore, we explored the effects of modifying the 5-position of the indole with a group that would add polarity at physiological pH. Because our previous SAR studies showed that there was some flexibility at the 5-position of the indole ring (compare compounds **13** and **14**), we designed an analogue of **14** that added charge and also included a methyl at the indole's 2-position. We envisaged that the OH analogue **21** could be alkylated with methyl 4-(bromomethyl)benzoate, which could then be hydrolyzed to its acid to provide a highly water-soluble analogue at pH 7.4. However, we were somewhat surprised that no appreciable amount of product could be produced by direct alkylation of **21**. Multiple bases were screened with varying pK_a values, from K_2CO_3 and Cs_2CO_3, as well as triethylamine, tetramethylguanidine, 1,8-diazabicyclo[5.4.0]undec-7-ene (DBU), and NaH. In all reactions, alkylation at the pyridine nitrogen was observed. Stronger bases such as TMG and NaH, even using 1 equiv, produced appreciable indole-N-alkylation as well as pyridine and indole-OH alkylation. The yield of singly alkylated product at the 5-indole position was negligible. Thus, a new route was designed by functionalizing the indole before introduction of the pyridine moiety (Scheme 2). Commercially available 2-methyl-5-methoxy-indole was demethylated with BBr_3 to provide **22**. Alkylation with 4-methyl-(bromomethyl)-benzoate under phase-transfer conditions afforded mono-O-alkylated

dx.doi.org/10.1021/jm201006x | J. Med. Chem. 2012, 55, 1940−1956

product **23**.[16] After formylation with $POCl_3$/DMF, intermediates **24** and **25** were independently prepared. Workup in mild base ($NaHCO_3$) produced the ester **24**, while workup in 5 N NaOH gave acid **25**. Condensations with 4-acetyl-pyridine provided the corresponding targets **26** and **27**. However, testing in glioblastoma cultures revealed that neither **26** nor **27** induced methuosis (Table 1).

Biological Activity of Compound 19 (MOMIPP) vs Compound 2 (MIPP). The foregoing studies identified compound **19** as the most potent for inducing methuosis. Hereafter, we refer to this compound by the acronym "MOMIPP" for 3-(5-methoxy, 2-methyl-1*H*-indol-3-yl)-1-(4-pyridinyl)-2-propen-1-one. Superior activity of MOMIPP versus compound **2** (MIPP) was confirmed in studies with U251 glioblastoma cells, using MTT viability assays, cell growth assays, morphological assessment, and colony-forming assays to compare MOMIPP and MIPP. Figure 2A shows the dose–response curves for the effects of the drugs on cell viability. Each compound was added at the indicated concentration for 2 days, with medium and compounds replenished after the first day. The relative IC_{50} for MOMIPP was 1.9 μM versus 4.8 μM for MIPP. To obtain a measure of the comparative duration of activity for each compound, their effects on cell growth and survival were assessed by counting the number of cells in parallel cultures treated for three consecutive days with 2.5, 5, or 10 μM compound (Figure 2B). Unlike the viability studies, in these experiments, the compounds were added at the beginning of the study and were *not replenished* for the duration. Under these conditions, MOMIPP was clearly more effective than MIPP in reducing cell growth and viability. The reduction of cell number in the cultures treated with MOMIPP coincided with massive early vacuolization of the cells and loss of nonviable cells from the substratum (Figure 3A,B). In contrast, the cells treated with MIPP initially underwent vacuolization on days 1 and 2 but tended to recover, especially at the 2.5 μM concentration (Figure 3A). These studies demonstrate that a single application of MOMIPP has a much more sustained effect than MIPP on cell morphology and cell viability. The difference between the MOMIPP and the MIPP was underscored when colony-forming assays were used to evaluate proliferative capacity and long-term cell viability (Figure 4). MOMIPP was clearly more effective than MIPP in reducing colony formation when cells were treated for 2 days (Figure 4A). If treatment was shortened to just 4 h, MOMIPP was still more effective than MIPP, but higher concentrations of both compounds were required to reduce colony formation (Figure 4B).

To determine if the methuosis-inducing compounds might be effective for targeting TMZ-resistant glioblastoma, we used a previously generated TMZ-resistant U251 cell line that was essentially unaffected by concentrations of TMZ as high as 100 μM[10] (Figure 5A). As shown in Figure 5B, both MIPP and MOMIPP were able to induce methuosis and reduce cell viability in the TMZ-resistant cells, but the efficacy of MOMIPP was clearly superior to MIPP. The ability of MOMIPP to kill drug-resistant tumor cells by methuosis extends beyond glioblastoma. For example, we observed similar MOMIPP-induced vacuolization and loss of colony-forming ability in both parental and doxorubicin-resistant MCF-7 breast cancer cells (Figure 5C,D). To determine if the concentration of MOMIPP that is maximally toxic in cancer cells might also be cytotoxic to normal cells, we treated human mammary epithelial cells (HMEC) with 10 μM MOMIPP. As shown in Figure 5E, HMECs underwent extensive cytoplasmic vacuolization within 24 h after addition of MOMIPP. By 48 h, cell viability was reduced approximately 40% as compared with a 70% reduction seen in MCF7 breast carcinoma cells treated for the same period at a similar cell density (Figure 5F). To further assess the effects of MOMIPP on normal cells, we applied the compound to human skin fibroblasts. As in all of the other cell lines tested, 10 μM MOMIPP induced obvious vacuolization in the fibroblasts by 24 h (Figure 5G). Similar to the HMECs, normal fibroblasts plated at subconfluent density to maintain exponential growth during exposure to MOMIPP exhibited a 40% decline in viability by 48 h. However, when the fibroblasts were plated at a high initial density, so that they would be in stationary phase at the time that MOMIPP was added, cell viability was essentially unaffected (Figure 5H), even though the cells underwent vacuolization (not shown). These observations suggest that although MOMIPP can be cytotoxic

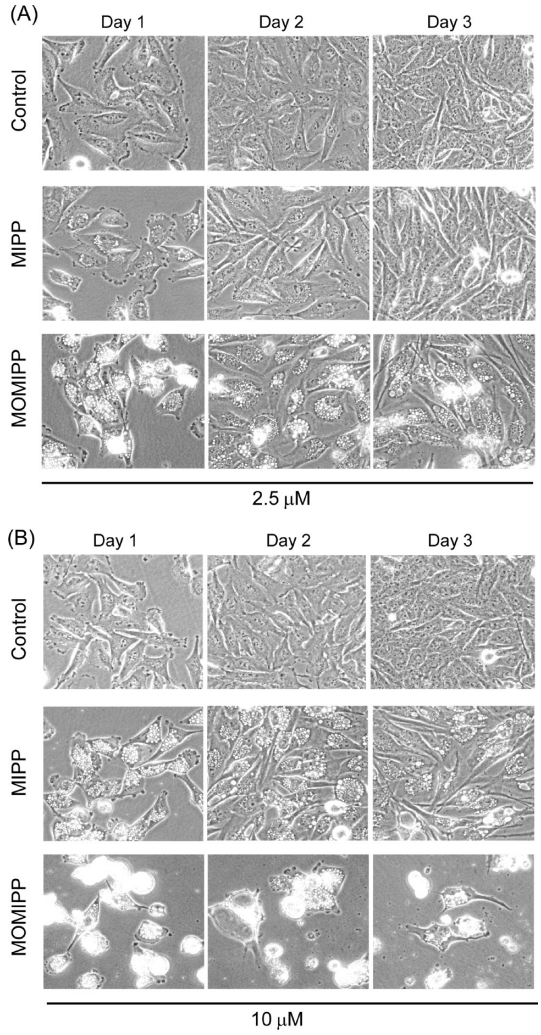

Figure 3. Comparison of the abilities of MOMIPP and MIPP to induce the morphological hallmarks of methuosis. One day after plating, U251 GBM cells were treated with MOMIPP or MIPP at final concentrations of 2.5 (A) or 10 μM (B). Controls received an equivalent volume of vehicle (DMSO). Cells were observed by phase contrast microscopy on three sequential days after addition of the compounds, without changing the medium or replenishing the compounds. Methuosis is characterized by extensive accumulation of phase-lucent cytoplasmic vacuoles, with eventual cell rounding and detachment from the substratum as viability is compromised.[6,10]

dx.doi.org/10.1021/jm201006x | *J. Med. Chem.* 2012, 55, 1940–1956

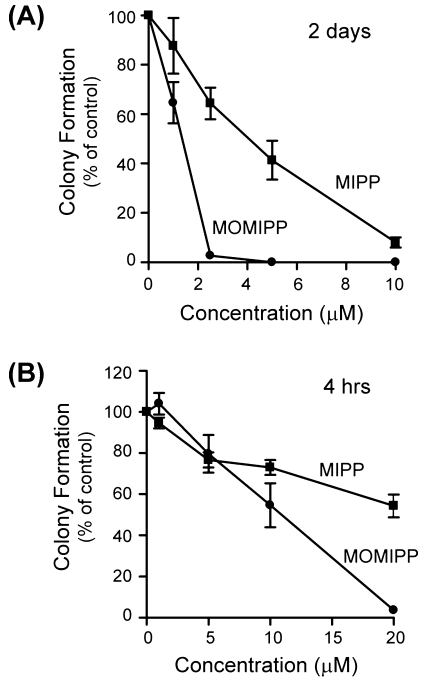

Figure 4. Comparison of the abilities of MOMIPP and MIPP to inhibit survival of U251 GBM cells in colony-forming assays. (A) Cells were plated for colony-forming assays as described in the Experimental Section. One day after plating the cells, MOMIPP (●) or MIPP (■) was added to the medium at the indicated concentrations, and cells were maintained in the presence of the compounds for 48 h. Thereafter, the compounds were removed, and colonies >50 cells were counted after 2 weeks. Each point represents the mean (±SD) from three separate dishes, with the results expressed as percent of the mean of the parallel control dishes containing DMSO. (B) The effects MOMIPP (●) and MIPP (■) on colony formation were compared as in panel A, except that cells were exposed to the compounds for only 4 h instead of 48 h.

to normal cells, the latter are somewhat less sensitive to the compound than the cancer cell lines, U251 and MCF7. A possible explanation for this is suggested by the differential effects of MOMIPP on subconfluent versus confluent fibroblasts, which imply that the disruptions of endosomal trafficking typified by vacuolization may be relatively well tolerated in cells that are not dividing as compared with cells that are actively proliferating.

Synthesis and Biological Activity of Potential Photoaffinity Labels. Our SAR studies showed that very subtle changes to the structures of MIPP or MOMIPP (e.g., modifications of the pyridine ring) can abolish their capacity to induce methuosis. Although chalcones are widely recognized as electrophiles, the level of structural specificity required for induction of methuosis suggests that the immediate effects of MIPP and MOMIPP are most likely due to their interactions with one or more distinct molecular targets. Several examples of protein-specific modifications by electrophilic compounds have been reported (see the Discussion). Therefore, an important goal for the future is to identify the targets of methuosis-inducing chalcones. A common approach for identifying drug targets is affinity chromatography.[17] However, at this point, our SAR studies have not revealed any nonessential sites that could be linked to a bulky affinity tag (e.g., biotin) or tethered to a solid matrix without loss of activity. Therefore, we focused on generating minimally modified biologically active analogues with reactive groups that might be useful for photoaffinity-based drug target discovery efforts.[18]

Initially, we designed a pseudobenzophenone analogue of MIPP as a potential photoaffinity probe. Benzophenones are commonly incorporated into active molecules for target identification studies.[18−21] On the basis of the structure of compound **14**, we postulated that a 5-benzoyl analogue might retain activity and function as a photoaffinity probe. The benzophenone analogue (compound **30**, benzoyl-MIPP) was prepared in two steps, starting with acylation of the Vilsmeier−Haack intermediate of 2-methylindole (Scheme 3A). With unmethylated indole, this system has been shown to direct acylation to the 5- and 6-positions.[22] In our hands, acylation of the Vilsmeier−Haack intermediate of 2-methylindole gave a 1:3 mixture of 5- and 6-benzoyl-2-methylindole-3-carboxaldehyde, respectively (**28** and **29**). This regioselectivity was characterized by 1D nuclear Overhauser effect (NOE) as described in the Experimental Section. In the second step of the scheme, the final compounds **30** and **31** were made by coupling the aldehydes with 4-acetyl pyridine in the presence of piperidine. Subsequent morphology and viability studies revealed that unlike the benzyloxy derivative (compound **14**), neither of the benzophenone analogues (**30** and **31**) induced methuosis when tested in U251 cells (data not shown).

Aromatic azides represent another photoreactive moiety commonly used in photoaffinity labeling.[18,23−25] Thus, we next explored the possibility that an azide could be added to either the 5- or the 6-position of the indole ring without loss of methuosis-inducing activity, as the azide represents less of a structure change from MOMIPP than the benzoyl group of compound **30**. The synthesis of compound **36** (5-azido MIPP) was based on the directed nitration of 2-alkylindoles toward the 5-position,[26] with further conversion to an azide by diazotization (see Scheme 3B). 2-Methylindole was selectively nitrated in concentrated sulfuric acid to yield **32** (see the Experimental Section details for validation of regiospecificity), which was then hydrogenated to amine **33**. Under mild diazotization conditions, the aminoindole was converted to the aromatic azide **34**.[27] The azide was formylated to obtain **35** and condensed with 4-acetyl-pyridine, providing **36**, 5-azido-MIPP. Separately, the same reaction scheme was performed on 2-methyl-5-methoxyindole, wherein nitration led predominately to the 6-nitrated product **37**. The same sequence of reaction steps described above was then completed to obtain **41**, 6-azido-MOMIPP.

Evaluation of the biological activities of **36** (5-azido MIPP) and **41** (6-azido MOMIPP) indicated that both compounds retained methuosis-inducing activity as judged by both cellular vacuolization (Figure 6A) and inhibition of colony formation (Figure 6B,C) in U251 cells. Although not as potent as MOMIPP, the 5-azido compound was clearly superior to the 6-azido compound in terms of its biological activity.

■ DISCUSSION

Methuosis is a newly discovered form of nonapoptotic cell death that is triggered by alterations of macropinocytotic vesicular trafficking, resulting in massive cellular vacuolization and loss of cellular metabolic integrity.[6] We recently described MIPP as a chalcone-like small molecule that is capable of inducing methuosis in GBM and other cancer cell lines.[10] Here, we present SAR studies that have led to the identification of a 5-methoxy analogue termed MOMIPP, which demonstrates improved potency and stability in cell culture systems. We have

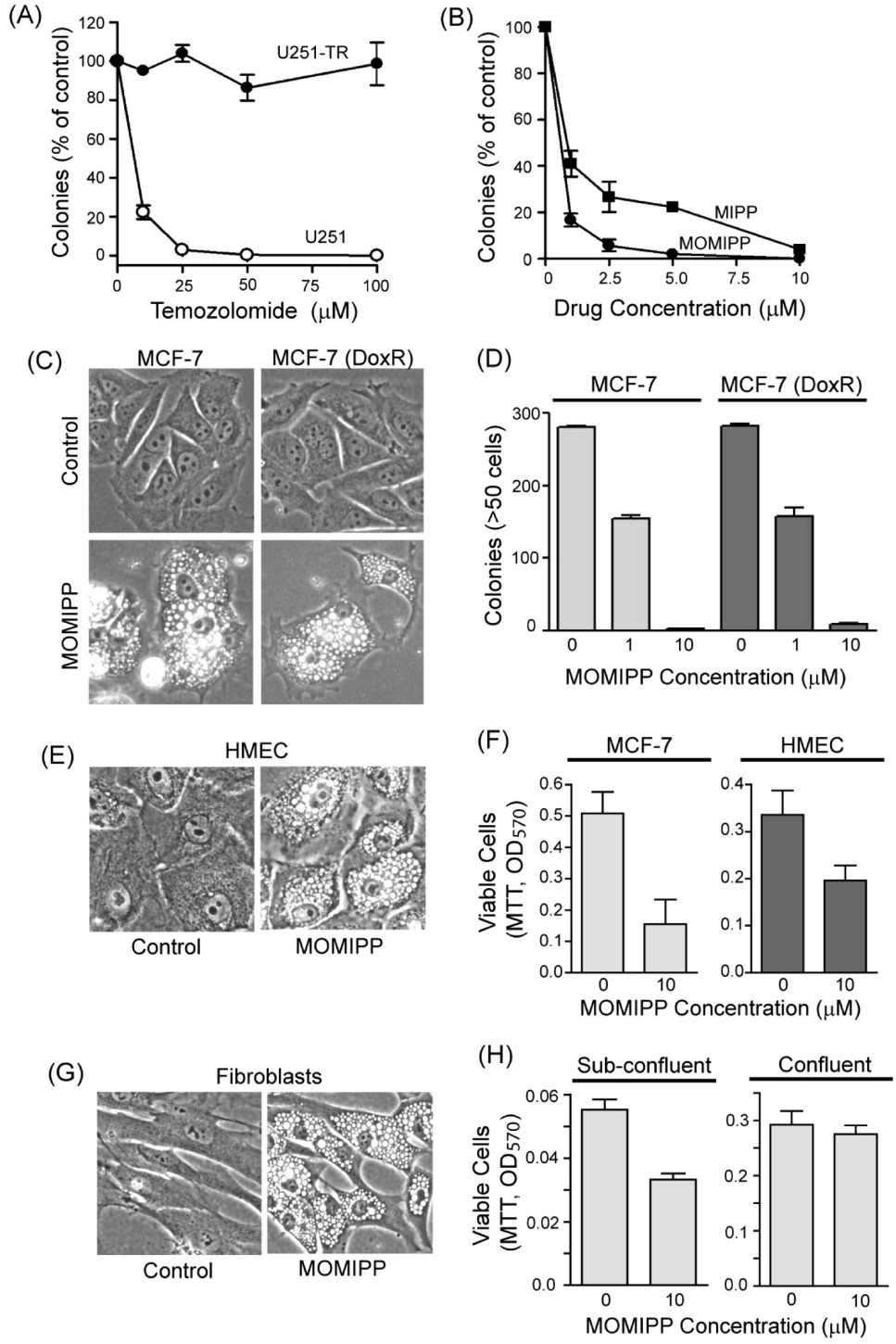

Figure 5. MOMIPP effectively inhibits the viability of drug-resistant GBM and breast cancer cells. (A) TMZ-resistant U251 glioblastoma cells (U251-TR) were derived as described previously.[10] The graph, reprinted from ref 10 with permission, shows that in contrast to the parental U251 cells, the viability of U251-TR cells is not reduced by treatment with TMZ. (B) The U251-TR cells were treated with the indicated concentrations of MIPP or MOMIPP for 48 h and then subjected to colony-forming assays as described in the Experimental Section. Each point is based on colony counts from three dishes (mean ± SD), with the results expressed as percent of the mean from parallel control dishes treated with an equivalent volume of vehicle alone (DMSO). (C) Parental and doxorubicin-resistant (DoxR) MCF-7 breast cancer cells[56] were treated with 10 μM MOMIPP for 24 h and then examined by phase-contrast microscopy. (D) Long-term viability of parental or DoxR MCF-7 cells was assessed by colony-forming assay after a 48 h of treatment with the indicated concentrations of MOMIPP. The results are the mean ± SD of determinations performed on three parallel dishes. (E) Normal HMECs were treated with 10 μM MOMIPP or an equivalent volume of DMSO (control) and examined by phase-contrast microscopy after 24 h. (F) MCF-7 cells or HMECs were plated in 96-well plates. After 48 h, while the cells were still subconfluent, fresh medium containing 10 μM MOMIPP or an equal volume of vehicle (DMSO) was added. MTT viability assays were performed at a 48 h end point. Values are the means (±SD) from four separate wells. (G) Normal human skin fibroblasts were treated with 10 μM MOMIPP or an equivalent volume of DMSO (control) and examined by phase-contrast microscopy after 24 h. (H) Normal human fibroblasts were seeded in 96-well plates at subconfluent density (1000 cells/well) or confluent density (10000 cells/well). After 24 h, fresh medium containing 10 μM MOMIPP or an equal

dx.doi.org/10.1021/jm201006x | J. Med. Chem. 2012, 55, 1940–1956

Figure 5. continued

volume of vehicle (DMSO) was added. MTT viability assays were performed at a 48 h end point. Values are the means (±SD) from four separate wells.

Scheme 3. Synthesis of 5′ and 6′ Azido Derivatives of MIPP[a]

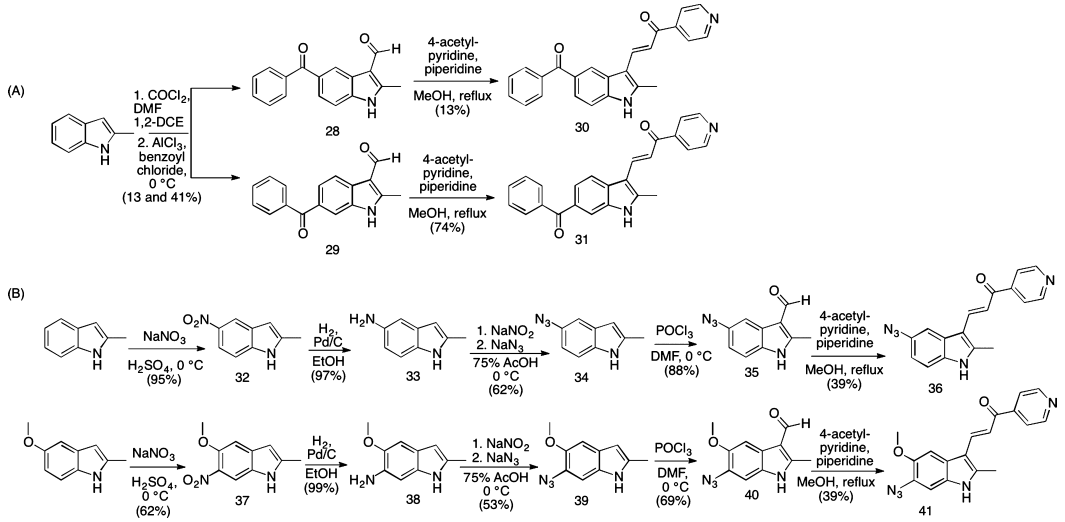

[a](A) Conditions and reagents: Compounds **28** and **29**: (1) $COCl_2$, DMF, 1,2-DCE, 0 °C; (2) $AlCl_3$, benzoyl chloride, 0 °C RT, 13 and 41% for **28** and **29**, respectively. Compound **30**: 4-acetyl-pyridine, piperidine, MeOH, reflux, 13%. Compound **31**: 4-acetyl-pyridine, piperidine, MeOH, reflux, 74%. (B) Conditions and reagents: Compound **32**: $NaNO_3$, H_2SO_4, 0 °C, 95%. Compound **33**: H_2, 10% Pd/C, EtOH, RT, 97%. Compound **34**: (1) $NaNO_2$; (2) NaN_3, 75% AcOH, 0 °C, 66%. Compound **35**: $POCl_3$, DMF, 0 °C, 88%. Compound **36**: 4-acetyl-pyridine, piperidine, MeOH, reflux, 39%. Compound **37**: $NaNO_3$, H_2SO_4, 0 °C, 62%. Compound **38**: H_2, 10% Pd/C, EtOH, RT, 99%. Compound **39**: (1) $NaNO_2$; (2) NaN_3, 75% AcOH, 0 °C, 53%. Compound **40**: $POCl_3$, DMF, 0 °C, 69%. Compound **41**: 4-acetyl-pyridine, piperidine, MeOH, reflux, 39%.

also generated active azido compounds that may be useful for future studies aimed at identifying the protein targets of MOMIPP.

In the course of generating a directed library of compounds for SAR studies, we carried out Claisen–Schmidt condensation reactions between various indole-3-carboxaldehydes and aromatic ketones catalyzed by piperidine, which efficiently provided indole-chalcones. As piperidine acts as a catalyst, we initially carried out the aldol condensations in the presence of catalytic amounts of piperidine. However, we generally observed higher yields when piperidine was used in excess. In almost all instances, the products precipitated from solution and were thus easily purified from excess catalyst (or starting material) by simple rinsing.

Our SAR studies provided several useful insights into the molecular features required for the methuosis-inducing activity of this class of compounds. First, regarding the indole ring, methylation of the nitrogen (compound **20**) or removal of the 2-methyl group (compound **13**) reduced but did not eliminate activity. At the 5-position, different modifications had opposite consequences. The activity of the 5-methoxy compound (**19**, MOMIPP) was substantially improved, and the 5-benzyloxy (compound **14**) was similar to unsubstituted MIPP. In contrast, modification of the 5-position with OH (compound **21**), *p*-methyl ester benzyloxyl (compound **26**), and *p*-COOH benzyloxyl (compound **27**) all caused a major loss of activity. Together, these findings demonstrate that there may be some flexibility at these positions on the indole ring for future attempts to further improve potency, create more water-soluble derivatives, or tether the compound to an affinity matrix. Regarding the second aryl system of the chalcone framework, we learned that the *para*-nitrogen orientation of the pyridine ring is critical for activity. Analogues with a 2-pyridine (compound **10**), 3-pyridine (compounds **11** and **16**), pyrazine (compound **17**), or phenyl (compound **9**) were inactive.

In considering the potential mechanisms through which MOMIPP induces cell death by methuosis, one possibility is that it could be acting as an electrophile (i.e., Michael acceptor). Compounds possessing electrophilic moieties that render them potential substrates to cellular nucleophiles are not often used in drug design because they can arbitrarily modify many biomolecules. This can lead to off-target effects, including the formation of immunoreactive haptens.[28] The SAR studies summarized in Table 1 show that while many of the compounds in our series possess the α,β-unsaturated ketone scaffold and could act as putative Michael acceptors, only MOMIPP and a few other compounds were effective inducers of methuosis at micromolar concentrations. Thus, it seems unlikely that MOMIPP is inducing cell death via general electrophilic modification of proteins. It remains possible that MOMIPP may be functioning as a target-specific Michael acceptor, with certain features of the molecule mediating association with a specific protein, where proximity of the α,β-unsaturated ketone to nucleophilic residues (e.g., cysteine) may then promote covalent modification. Examples of such protein-specific modifications have been reported for compounds that bind to the receptor protein ErbB2,[29] the TRPA1 ion channel,[30] the nuclear protein KSRP/FUBP2,[31] and sortase enzymes in Gram-positive bacteria.[32] These types of observations have spurred a general resurgence of interest in drugs that work by covalent modification of their specific targets.[33]

dx.doi.org/10.1021/jm201006x | *J. Med. Chem.* 2012, 55, 1940–1956

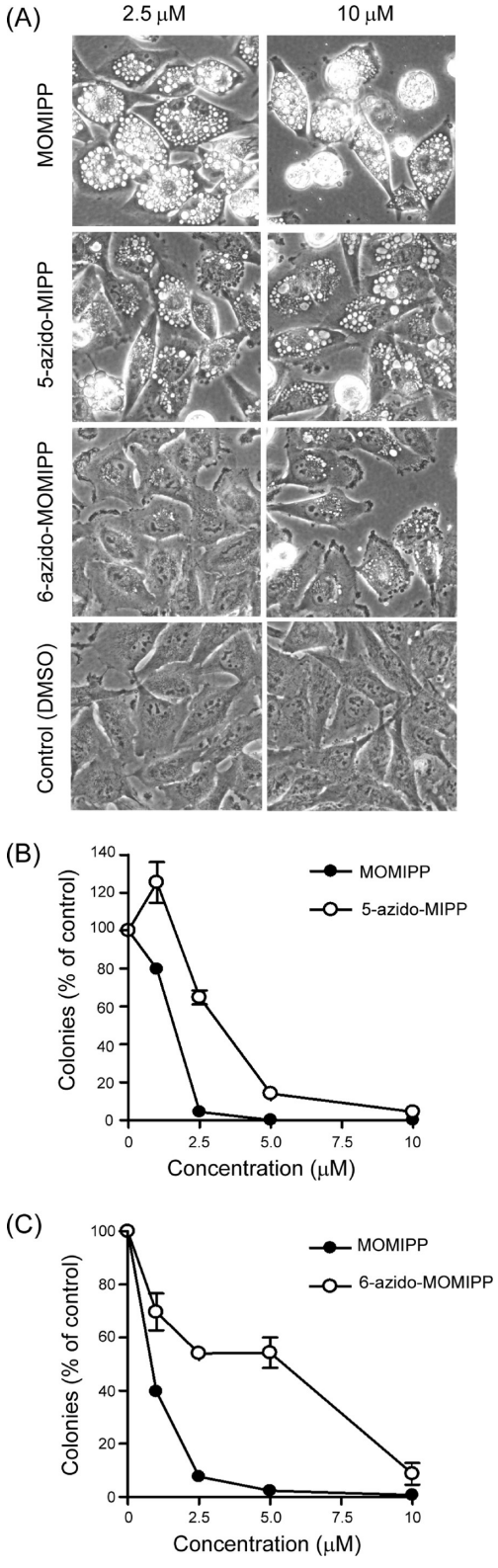

Figure 6. Comparison of the effects of MOMIPP (compound **19**), 5-azido-MIPP (compound **36**), and 6-azido-MOMIPP (compound **41**) on morphology and viability of U251 glioblastoma cells. (A) The indicated compounds were added to the cells at concentrations of 2.5 or 10 μM, and the cells were observed by phase-contrast microscopy after 48 h. (B and C) U251 cells were treated with varying concentrations of the indicated compounds for 48 h, and long-term cell viability was assessed by colony-forming assays. Each represents the counts from three dishes (mean ± SD), with the results expressed as percent of the mean from parallel control dishes treated with an equivalent volume of vehicle alone (DMSO).

Compounds broadly classified as chalcones have been shown to exhibit anticancer activity through multiple mechanisms, including disruption of p53 interactions with MDM2 or HDM2,[13,34] inhibition of p-glycoprotein,[35−37] and disruption of microtubule polymerization.[38−40] Many of the latter compounds were designed as analogues of colchicine and combretastatins, natural products known to bind β-tubulin. A number of publications have since established that chalcones and related molecules can act as antimitotic agents, and substantial progress has been made in understanding their SAR.[41,42] While our active methuosis-inducing compounds (e.g., MOMIPP) can be classified as chalcones, their specific features are quite distinct from most of the antimitotic chalcones previously described. The stringent structural specificity for induction of methuosis, with dependence on the specific substitution patterns of both the indolyl and the pyridinyl moieties, appears to differentiate MOMIPP from chalcones previously reported as antimitotic agents. We have not observed mitotic arrest prior to loss of viability in cells treated with these compounds (unpublished observation). Conversely, massive endosomal vacuolization akin to what we have observed with MOMIPP has not been reported with the antimitotic chalcones. Of all of the cytotoxic chalcones described in the literature, the one most related to MOMIPP contains an unsubstituted indole ring linked to a 3,4,5-trimethoxy phenyl moiety.[14] However, we found that replacement of the 4-pyridine of MOMIPP with a 3,4,5-trimethoxy phenyl group yielded a compound that did not induce appreciable cellular vacuolization or death when applied to U251 cells at 10 μM for 48 h (not shown). This is consistent with the lack of tolerance for modifications to the 4-pyridinyl moiety and suggests that the cytotoxicity previously reported for the trimethoxyphenyl indolyl chalcone[14] probably was not due to methuosis.

In general, cell death induced by antimitotic chalcones is thought to occur by classical apoptosis, not methuosis. A possible exception was noted in a recent report where a chalcone-derivative termed "C2" may have induced death in glioblastoma cells by a nonapoptotic mechanism involving accumulation of autophagic vacuoles.[43] However, as we have previously reported, the vacuoles induced during methuosis arise from macropinosomes and endosomes, which are distinct from autophagosomes.[6,10] It would be premature to rule out the possibility that MOMIPP might bind tubulin in a manner similar to colchicine and related chalcones, but so far, the preponderance of evidence suggests that the compounds described in this study act by a different mechanism to trigger abnormal macropinocytosis, swelling of endosomal compartments, and nonapoptotic cell death.[10] Ultimately, clarification of this mechanism will depend on identification of the specific molecular target(s) of MOMIPP and related compounds.

The future identification of the specific target(s) of MOMIPP will be important for several reasons: (1) The expression level or activity of the identified target(s) might have predictive value for determining which types of tumors would be most susceptible to the compound, (2) understanding the function(s) of the proteins targeted by MOMIPP could be helpful for assessing the potential toxicity to normal cells, and

dx.doi.org/10.1021/jm201006x | J. Med. Chem. 2012, 55, 1940−1956

(3) knowledge about the target protein(s) will facilitate analysis of the drug binding site that could suggest modifications to increase potency or specificity. In this respect, our finding that incorporation of a photoreactive azide at the 5-position of the indole ring of MIPP yields a derivative that retains good methuosis-inducing activity (Figure 6) offers several avenues for protein target identification using established strategies. Aside from the photoreactive azide **36**, MOMIPP's core structure contains two other features that may render it suitable for target identification studies, potentially bypassing the need for incorporation of a photoreactive azide. First, MOMIPP itself may be photoreactive and could behave similarly to an excited benzophenone. The core scaffold of MOMIPP is a pseudodiarylketone (as one side contains a double vinylogous amide through the indole, while the other contains a 4-pyridine) and could potentially exhibit photoexcitation chemistry similar to that of a benzophenone. We are currently pursuing experiments to characterize MOMIPP's inherent photoreactivity and its ability to insert into other molecules. The second characteristic of MOMIPP's core structure that may render it suitable for target identification is its electrophilic α,β-unsaturated ketone moiety, which may be responsible for a covalent modification of a nucleophilic target residue (e.g., cysteine). Thus, if MOMIPP is covalently binding to its target protein(s), there may be no need for photoinitiated reactive intermediate formation. This possibility is also undergoing further study.

The key observation that MOMIPP effectively induced methuosis in TMZ-resistant GBM cells, as well as doxorubicin-resistant breast cancer cells, raises the possibility that further development of this compound could lead to useful therapeutic agents for treating cancers that are resistant to drugs that commonly work by inducing apoptosis. Ultimately, deployment of MOMIPP or related compounds as anticancer agents will need to address some challenges. Preliminary studies indicate that MOMIPP's ability to induce vacuolization is not restricted to cancer cells (Figure 5E−H). However, the studies with normal HMECs and skin fibroblasts suggest that the consequences of vacuolization for cell viability are more severe for rapidly dividing cancer cells than normal cells, particularly when the normal cells enter stationary phase at high cell density (Figure 5H). This raises a possibility that a therapeutic window might be identified for selective effects on cancer cells. A second challenge relates to the poor aqueous solubility of MOMIPP and most of its active analogues. However, similar solubility issues have been encountered with other hydrophobic anticancer drugs (e.g., taxol, camptothecin) and have been circumvented through the use of appropriate excipients[44] or novel nanoparticle[45,46] or liposome[47,48] based delivery strategies. The latter strategies may offer the additional benefit of allowing selective targeting of nonspecific agents by surface modification of the delivery vehicle with tumor-specific peptides or antibodies.[45,49,50] Thus, given the observed cytotoxic affects of MOMIPP on drug-resistant cancer cells and the range of available options for its delivery in vivo, we believe that MOMIPP can serve as a valuable prototype for further preclinical testing.

EXPERIMENTAL SECTION

Chemistry. *General Methods.* Reagents and starting materials were obtained from commercial suppliers without further purification. Thin-layer chromatography (TLC) was done on 250 μm fluorescent silica gel 1B−F plates and visualized with UV light. Flash column chromatography was performed using silica gel 230−400 μm mesh size. Melting points (MP) are uncorrected. Nuclear magnetic resonance (NMR) spectra were recorded on either a 600, 400, or 200 MHz instrument. Peak locations were referenced using the residual solvent peak [7.26 and 77.16 for $CDCl_3$ ^1H and ^{13}C, respectively, and 2.50 and 39.51 for dimethylsulfoxide (DMSO) ^1H and ^{13}C]. Proton coupling constants (J values) and signals are expressed in hertz using the following designations: s (singlet), d (doublet), br s (broad singlet), m (multiplet), t (triplet), dd (doublet of doublets), and qd (quintet of doublets). NMR spectra are available in the Supporting Information. All synthesized compounds were at least 95% pure as determined by elemental analysis (Atlantic Microlabs, Norcross, GA).

*2-Methylindole-3-carboxaldehyde (**2a**).*[51] To a dried 300 mL two-neck round-bottom flask under argon at 0 °C, *N*,*N*-DMF (3 mL) was added, followed by $POCl_3$ (1.05 mL, 11.3 mmol). After this was stirred for 10 min, 2-methylindole (1.23 g, 9.37 mmol) dissolved in DMF (6 mL) was added dropwise via an addition funnel under argon. After 2 h, 1 N NaOH (70 mL) was added slowly, upon which a white precipitate formed. The solid was filtered and dried under vacuum, yielding 1.32 g (89%) of white solid. ^1H NMR (600 MHz, d_6-DMSO): δ 11.998 (s, 1H, N−H), 10.050 (s, 1H, CHO), 8.044−8.032 (d, J = 7.2, 1H, indole-4H), 7.388−7.375 (d, J = 7.8, 1H, indole-7H), 7.183−7.135 (m, 2H, indole-5,6H), 2.679 (s, 3H, methyl). ^{13}C NMR (150 MHz, d_6-DMSO): δ 184.3, 148.6, 135.4, 125.6, 122.7, 121.9, 120.0, 113.7, 111.4, 11.5. Melting point: 195−200 °C (published:[51] 197−200 °C). TLC (ethyl acetate:hexanes 4:1) R_f = 0.39. Elemental analysis calculated for $C_{10}H_9NO$: C, 75.45; H, 5.70; N, 8.80. Found: C, 75.23; H, 5.70; N, 8.93.

*trans-3-(2-Methyl-1H-indol-3-yl)-1-(4-pyridinyl)-2-propen-1-one (**2**).*[52] To a dried 500 mL round-bottom flask under argon, 2-methylindole-3-carboxaldehyde (400 mg, 2.51 mmol) was dissolved in anhydrous MeOH (10 mL). 4-Acetyl-pyridine (305 μL, 2.76 mmol, 1.1 equiv) and piperidine (82 μL, 0.83 mmol) were added, and the reaction was stirred under reflux. A red-orange precipitate gradually formed, and after 12 h, this solid was isolated by filtration, rinsed with chilled methanol, and dried under vacuum, producing 458 mg (69%) of yellow solid. NMR: ^1H NMR (600 MHz, d_6-DMSO): δ 12.017 (s, 1H, N−H), 8.816−8.806 (dd, J_1 = 4.5, J_2 = 2.1, 2H, pyr-2,6H), 8.121−8.095 (d, J = 15.6, 1H, C═CH), 8.077−8.063 (m, 1H, indole-4H), 7.975−7.965 (dd, J_1 = 4.5, J_2 = 1.5, 2H, pyr-3,5H), 7.489−7.464 (d, J = 15.6, 1H, C═CH), 7.415−7.400 (m, 1H, indole-7H), 7.220−7.200 (m, 2H, indole-5,6H), 2.596 (s, 3H, methyl). ^{13}C NMR (150 MHz, d_6-DMSO): δ 188.0, 150.7, 145.6, 144.9, 139.5, 136.3, 125.8, 122.4, 121.50, 121.46, 120.4, 113.1, 111.7, 109.4, 11.9. Melting point: 268−272 °C. TLC (ethyl acetate:hexanes 4:1) R_f = 0.18. Elemental analysis calculated for $C_{17}H_{14}N_2O$: C, 77.84; H, 5.38; N, 10.68. Found: C, 77.96; H, 5.28; N, 10.59.

*trans-3-(1H-Indol-3-yl)-1-phenyl-2-propen-1-one (**9**).*[15] In a dried, 25 mL round-bottom flask under argon, indole-3-carboxaldehyde (300 mg, 2.07 mmol) was dissolved in anhydrous methanol (8 mL). Acetophenone (240 μL, 2.07 mmol) and piperidine (100 μL, 1.00 mmol) were added. The reaction was stirred under reflux for 18 h. Ten percent acetic acid was added (10 mL), precipitating 248 mg of a crude yellow solid. This was recrystallized in 100% EtOH, filtered, and dried under vacuum, yielding a pure, yellow solid (198 mg, 39%, 247.29 MW). ^1H NMR (600 MHz, d_6-DMSO): δ 8.133−8.114 (m, 3H, phenyl-2,6H, indole-2H), 8.095−8.081 (m, 1H, indole-4H), 8.075−8.049 (d, J = 15.6, 1H, C═CH), 7.668−7.642 (d, J = 15.6, 1H, C═CH), 7.655−7.629 (m, 1H, phenyl-4H), 7.581−7.556 (t, J = 1.5, 2H, phenyl-3,5H), 7.504−7.490 (m, 1H, indole-7H), 7.254−7.231 (m, 2H, indole-5,6H). ^{13}C NMR (150 MHz, d_6-DMSO): δ 188.8, 139.1, 138.5, 137.5, 133.4, 132.4, 128.7, 128.2, 125.1, 122.8, 121.2, 120.4, 115.3, 112.8, 112.5. Melting point: 167−170 °C (published:[15] 166−167 °C). TLC (in 2:1 ethyl acetate:hexanes) R_f = 0.48. Elemental analysis calculated for $C_{17}H_{13}NO$: C, 82.57; H, 5.30; N, 5.66. Found: C, 82.19; H, 5.35; N, 5.63.

*trans-3-(1H-Indol-3-yl)-1-(2-pyridinyl)-2-propen-1-one (**10**).*[52] Indole-3-carboxaldehyde (200 mg, 1.38 mmol) was added to a dried 100 mL round-bottom flask under argon, and anhydrous methanol (8 mL) was added. 2-Acetyl-pyridine (232 μL, 2.07 mmol) and piperidine (69 μL, 0.7 mmol) were added, and the reaction was stirred under reflux for 24 h, after which still no precipitate had formed (AcOH did not lead to precipitation). The crude reaction mixture was concentrated and directly applied to a silica column for chromatography (ethyl acetate:hexanes 1:1). The product was partially separated from the aldehyde starting material (some product coeluted with aldehyde and was discarded), and 80 mg (23%) of purified product was isolated. NMR: ^{1}H NMR (600 MHz, d_6-DMSO): δ 11.989 (s, 1H, N−H), 8.831−8.819 (m, pyr-H2), 8.220−8.194 (d, J = 15.6, 1H, C═CH), 8.154−8.105 (m, 3H, C═CH, indole-H2, pyr-H3), 8.052−8.027 (m, 1H, pyr-H4), 7.976−7.962 (m, 1H, indole-H4), 7.679−7.656 (m, 1H, pyr-H5), 7.522−7.508 (m, 1H, indole-H7), 7.285−7.262 (m, 2H, indole-H5,6). ^{13}C NMR (150 MHz, d_6-DMSO): δ 188.2, 154.3, 149.1, 139.3, 137.7, 137.6, 134.2, 127.1, 125.1, 122.3, 122.2, 121.4, 120.1, 114.3, 113.1, 112.7. Melting point: 141−145 °C. TLC (ethyl acetate:hexanes 4:1) R_f = 0.40. Elemental analysis calculated for $C_{16}H_{12}N_2O{\cdot}0.1C_4H_8O_2$: C, 76.62; H, 5.02; N, 10.90. Found: C, 76.41; H, 5.03; N, 10.80.

*trans-3-(1H-Indol-3-yl)-1-(3-pyridinyl)-2-propen-1-one (**11**).*[53] Indole-3-carboxaldehyde (100 mg, 0.69 mmol) was added to a dried 100 mL round-bottom flask and dissolved in anhydrous methanol (5 mL). 3-Acetyl-pyridine (113 μL, 1.03 mmol, 1.5 equiv) and piperidine (69 μL, 0.7 mmol) were added, and the reaction was stirred under reflux. After 12 h, the reaction was cooled to room temperature, upon which a precipitate formed. The solid was filtered, yielding 54 mg. However, there was significant aldehyde present on a crude NMR. This mixture was dry-loaded onto silica and purified by column chromatography (methylene chloride:methanol 9:1), producing 33 mg of pure, yellow solid (19%). NMR: ^{1}H NMR (600 MHz, d_6-DMSO): δ 12.004 (s, 1H, N−H), 9.292−9.289 (d, J = 1.8, 1H, pyr-H2), 8.808−8.797 (dd, J_1 = 4.8, J_2 = 1.8, 1H, pyr-H6), 8.467−8.447 (dt, J_1 = 7.8, J_2 = 2.1, 1H, pyr-H4), 8.174 (s, 1H, indole-H2), 8.154−8.140 (dd, J_1 = 6.6, J_2 = 1.8, 1H, indole-H4), 8.120−8.095 (d, J = 15.0, 1H, C═CH), 7.665−7.639 (d, J = 15.6, 1H, C═CH), 7.607−7.585 (m, 1H, pyr-H5), 7.506−7.492 (dd, J_1 = 6.9, J_2 = 1.5, 1H, indole-H7), 7.268−7.223 (qd, J_1 = 6.6, J_2 = 1.5, 1H, indole-H5,6). ^{13}C NMR (150 MHz, d_6-DMSO): δ 187.9, 152.7, 149.3, 139.9, 137.6, 135.7, 134.1, 133.7, 125.1, 123.9, 122.9, 121.3, 120.7, 115.0, 112.9, 112.5. Melting point: 192−194 °C (published:[53] 191 °C). TLC (methylene chloride:methanol 9:1) R_f = 0.26. Elemental analysis calculated for $C_{16}H_{12}N_2O$: C, 77.40; H, 4.87; N, 11.28. Found: C, 77.00; H, 4.80; N, 11.12.

*trans-3-(1H-Indol-3-yl)-1-(4-pyridinyl)-2-propen-1-one (**12**).*[53] In a dried, 25 mL round-bottom flask under argon, indole-3-carboxaldehyde (300 mg, 2.07 mmol) was dissolved in anhydrous methanol (8 mL). 4-Acetyl-pyridine (229 μL, 2.07 mmol) and piperidine (100 μL, 1.00 mmol) were added. The reaction was stirred under reflux; gradually, yellow product precipitated during the reaction. After 14 h, the reaction was cooled to room temperature, filtered, and washed with chilled methanol and hexanes. Drying under vacuum for 2 h yielded a pure, yellow solid (343 mg, 67%). ^{1}H NMR (600 MHz, d_6-DMSO): δ 8.826−8.816 (dd, J_1 = 4.2, J_2 = 1.8, 2H, pyr-H2,6), 8.186−8.182 (d, J = 2.4, 1H, indole-H2), 8.128−8.117 (m, 1H, indole-H4), 8.121−8.095 (d, J = 15.6, 1H, C═CH), 7.978−7.968 (dd, J_1 = 4.2, J_2 = 1.8, 2H, pyr-H3,5), 7.592−7.566 (d, J = 15.6, 1H, C═CH), 7.512−7.498 (m, 1H, indole-H7), 7.267−7.243 (m, 2H, indole H-5,6). ^{13}C NMR (150 MHz, d_6-DMSO): δ 188.4, 150.7, 144.7, 140.9, 137.6, 134.6, 125.0, 123.0, 121.5, 121.4, 120.6, 114.6, 112.9, 112.6. Melting point: 266−268 °C (published:[53] 257−258 °C). TLC (in 4:1 ethyl acetate:hexanes) R_f = 0.23. Elemental analysis calculated for $C_{16}H_{12}N_2O$: C, 77.40; H, 4.87; N, 11.28. Found: C, 77.35; H, 4.84; N, 11.23.

*trans-3-(5-Methoxy-1H-indol-3-yl)-1-(4-pyridinyl)-2-propen-1-one (**13**).* In a dried, 25 mL round-bottom flask under argon, 5-methoxyindole-3-carboxaldehyde (100 mg, 0.57 mmol) was dissolved in anhydrous methanol (3 mL). 4-Acetyl-pyridine (63 μL, 0.57 mmol) and piperidine (30 μL, 0.3 mmol) were added. The reaction was stirred under reflux, during which a crude yellow solid precipitated. After 15 h, 10% acetic acid (10 mL) was added to further the precipitation. The solid was filtered and dried under vacuum, yielding a pure, yellow solid (121 mg, 76%). ^{1}H NMR (600 MHz, d_6-DMSO): δ 8.821−8.811 (dd, J_1 = 4.5, J_2 = 1.5, 2H, pyr-H2,6), 8.163−8.159 (d, J = 2.4, 1H, indole-H2), 8.117−8.091 (d, J = 15.6, 1H, C═CH), 7.953−7.943 (dd, J_1 = 4.5, J_2 = 1.5, 2H, pyr-H3,5), 7.532−7.506 (d, J = 15.6, 1H, C═CH), 7.489−7.485 (d, J = 2.4, 1H, indole-H4), 7.405−7.391 (d, J = 8.4, 1H, indole-H7), 6.902−6.883 (dd, J_1 = 9.0, J_2 = 2.4, 1H, indole-H6), 3.866 (s, 3H, methyl). ^{13}C NMR (150 MHz, d_6-DMSO): δ 188.4, 155.2, 150.7, 144.9, 140.9, 134.2, 132.4, 126.0, 121.5, 114.3, 113.3, 112.7, 112.4, 102.4, 55.6. Melting point: 235−237 °C. TLC (in 4:1 ethyl acetate:hexanes) R_f = 0.20. Elemental analysis calculated for $C_{17}H_{14}N_2O_2$: C, 73.37; H, 5.07; N, 10.07. Found: C, 73.55; H, 5.00; N, 10.04.

*trans-3-(5-Phenylmethoxy-1H-indol-3-yl)-1-(4-pyridinyl)-2-propen-1-one (**14**).* In a dried, 25 mL round-bottom flask under argon, 5-benzyloxyindole-3-carboxaldehyde (100 mg, 0.40 mmol) was dissolved in anhydrous methanol (3 mL). 4-Acetyl-pyridine (75 μL, 0.68 mmol) and piperidine (20 μL, 0.2 mmol) were added. The reaction was stirred under reflux, during which a crude yellow solid precipitated. The solid was filtered, rinsed with cold methanol, and dried under vacuum. This crude product (107 mg) was purified from residual aldehyde by column chromatography in ethyl acetate:hexanes (1:1 → 3:1 gradient), yielding pure, yellow solid (70 mg, 49%). ^{1}H NMR (600 MHz, d_6-DMSO): δ 8.837−8.827 (dd, J_1 = 4.5, J_2 = 1.5, 2H, pyr-2,6H), 8.148−8.143 (d, J = 3.0, 1H, indole-2H), 8.095−8.069 (d, J = 15.6, 1H, C═CH), 7.932−7.922 (dd, J_1 = 4.5, J_2 = 1.5, 2H, pyr-3,5H), 7.556−7.553 (d, J = 1.8, 1H, indole-4H), 7.523−7.511 (d, J = 7.2, 2H, phenyl-2,6H), 7.460−7.434 (d, J = 15.6, 1H, C═CH), 7.411−7.370 (m, 3H, phenyl-3,5H, indole-7H), 7.330−7.306 (t, J = 7.2, 1H, phenyl-4H), 6.979−6.961 (dd, J_1 = 8.4, J_2 = 2.4, 1H, indole-6H), 5.252 (s, 2H, methylene). ^{13}C NMR (150 MHz, d_6-DMSO): 188.4, 154.1, 150.7, 144.9, 140.9, 137.7, 134.6, 132.5, 128.4, 127.7, 127.6, 125.8, 121.5, 114.2, 113.3, 113.1, 112.7, 104.1, 69.8. Melting point: 218−221 °C. TLC (in 4:1 ethyl acetate:hexanes) R_f = 0.26. Elemental analysis calculated (for $C_{23}H_{19}N_2O_2{\cdot}0.2C_6H_{14}{\cdot}0.05H_2O$): C, 78.02; H, 5.93; N, 7.52. Found: C, 77.69; H, 5.62; N, 7.24.

*trans-3-(5-Hydroxy-1H-indol-3-yl)-1-(4-pyridinyl)-2-propen-1-one (**15**).* To a dried two-neck 250 mL round-bottom flask under argon at −40 °C, **13** (352 mg, 0.99 mmol) was partially dissolved in CH_2Cl_2 (30 mL). BBr_3 (10 mL, 1.0 M in CH_2Cl_2, 10 mmol) was added dropwise via an addition funnel under argon. After 4 h, the reaction was poured onto ice and treated with 5 N NaOH until pH ≈ 12. The aqueous solution was isolated and treated with 5 N HCl until pH ≈ 7, forming a brown precipitate, which was extracted with ethyl acetate (3 × 40 mL). Extracts were combined, dried with Na_2SO_4, filtered, concentrated, and dried under vacuum to yield 158 mg of an orange solid (61%). NMR: ^{1}H NMR (600 MHz, d_6-DMSO): δ 11.840 (s, 1H, N−H), 9.109 (s, 1H, O−H), 8.826−8.816 (dd, J_1 = 4.5, J_2 = 1.5, 2H, pyr-2,6H), 8.063−8.058 (d, J = 3.0, 1H, indole-2H), 8.048−8.022 (d, J = 15.6, 1H, C═CH), 7.902−7.892 (dd, J_1 = 4.5, J_2 = 1.5, 2H, pyr-3,5H), 7.349−7.346 (d, J = 1.8, 1H, indole-4H), 7.307−7.293 (d, J = 8.4, 1H, indole-H7), 6.762−6.744 (dd, J_1 = 8.4, J_2 = 2.4, 1H, indole-H6). ^{13}C NMR (150 MHz, d_6-DMSO): δ 188.2, 152.9, 150.6, 145.0, 141.4, 134.8, 131.7, 126.0, 121.3, 113.6, 113.1, 112.7, 112.3, 104.9. Melting point: 262−268 °C. TLC (in ethyl acetate:hexane 4:1) R_f = 0.35. Elemental analysis calculated for $C_{16}H_{12}N_2O_2{\cdot}0.1H_2O$: C, 72.22; H, 4.62; N, 10.53. Found: C, 72.21; H, 4.42; N, 10.26.

*trans-3-(5-Methoxy-1H-indol-3-yl)-1-(3-pyridinyl)-2-propen-1-one (**16**).* In a dried, 50 mL round-bottom flask under argon, 5-methoxyindole-3-carboxaldehyde (100 mg, 0.57 mmol) was dissolved in anhydrous methanol (4 mL). 3-Acetyl-pyridine 63 μL, 0.57 mmol) and piperidine (30 μL, 0.30 mmol) were added. The reaction was stirred under reflux, during which a crude orange solid precipitated. After 20 h, the solid was isolated by vacuum filtration, rinsed with chilled methanol, and dried under vacuum, yielding a pure, orange solid (98 mg, 60%). ^{1}H NMR (600 MHz, d_6-DMSO): δ 11.891 (s, 1H, N−H), 9.276−9.273 (d, J = 1.8, 1H, pyr-2H), 8.798−8.790 (m, 1H, pyr-6H), 8.440−8.421 (m, 1H, pyr-4H), 8.155−8.150 (d, J = 3.0, 1H,

indole-2H), 8.113−8.088 (d, J = 15.0, 1H, C═CH), 7.607−7.582 (d, J = 15.0, 1H, C═CH), 7.598−7.584 (m, 1H, pyr-5H), 7.500−7.497 (d, J = 1.8, 1H, indole-4H), 7.397−7.383 (d, J = 8.4, 1H, indole-7H), 6.892−6.874 (dd, J_1 = 8.4, J_2 = 2.4, 1H, indole-6H), 3.867 (s, 3H, methyl). ^{13}C NMR (150 MHz, d_6-DMSO): δ 187.9, 155.1, 152.6, 149.3, 139.9, 135.7, 133.8, 133.7, 132.3, 126.1, 123.9, 114.7, 113.2, 112.7, 112.4, 102.6, 55.6. Melting point: 169−173 °C. TLC (in 4:1 ethyl acetate:hexanes) R_f = 0.17. Elemental analysis calculated $C_{17}H_{14}N_2O_2$: C, 73.37; H, 5.07; N, 10.07. Found: C, 73.09; H, 5.10; N, 10.01.

*trans-3-(5-Methoxy-1H-indol-3-yl)-1-(pyrazine)-2-propen-1-one (**17**).* In a dried, 25 mL round-bottom flask under argon, 5-methoxyindole-3-carboxaldehyde (75 mg, 0.43 mmol) was dissolved in anhydrous methanol (4 mL). Acetyl-pyrazine (52 mg, 0.43 mmol) and piperidine (23 μL, 0.23 mmol) were added. The reaction was stirred under reflux, during which a crude, yellow solid precipitated. After 3 h, the solid was isolated by vacuum filtration, rinsed with chilled methanol, and dried under vacuum. This crude product was recrystallized in EtOH (8 mL) to remove residual aldehyde, yielding a pure, yellow solid (28 mg, 24%). ^{1}H NMR (600 MHz, d_6-DMSO): δ 11.960 (s, 1H, N−H), 9.244 (s, 1H, pyr-2H), 8.905−8.873 (m, 2H, pyr-4,5H), 8.204−8.178 (d, J = 15.6, 1H, C═CH), 8.155 (s, 1H, indole-2H), 7.987−7.961 (d, J = 15.6, 1H, C═CH), 7.427−7.412 (m, 2H, indole-4,7H), 6.934−6.915 (dd, J_1 = 9.0, J_2 = 2.4, 1H, indole-6H), 3.853 (s, 3H, methyl). ^{13}C NMR (150 MHz, d_6-DMSO): δ 187.3, 155.1, 148.8, 147.6, 144.0, 143.7, 140.2, 134.6, 132.5, 126.0, 113.4, 113.2, 112.8, 111.9, 102.9, 55.6. Melting point: 176−180 °C. TLC (in 4:1 ethyl acetate:hexanes) R_f = 0.30. Elemental analysis calculated $C_{16}H_{13}N_3O_2$: C, 68.81; H, 4.69; N, 15.05. Found: 68.76; H, 4.64; N, 14.99.

*5-Methoxy-2-methyl-1H-indole-3-carboxaldehyde (**18**).*[54] To a dried two-neck 25 mL round-bottom flask at 0 °C, $POCl_3$ (1.00 mL, 10.8 mmol) was added to *N*,*N*-DMF (2.5 mL). After 10 min of stirring, 2-methyl-5-methoxyindole (1.45 mg, 9.00 mmol) dissolved in DMF (5 mL) was added dropwise. After 45 min, 1 N NaOH (50 mL) was slowly added, forming a white precipitate. The solid was isolated by filtration, washed with cold H_2O, and dried under vacuum, yielding 1.52 g of white solid (90%). ^{1}H NMR (600 MHz, d_6-DMSO): δ 11.875 (s, 1H, N−H), 10.009 (s, 1H, CHO), 7.570−7.566 (d, J = 2.4, 1H, indole-4H), 7.282−7.268 (d, J = 8.4, 1H, indole-7H), 6.797−6.778 (dd, J_1 = 9.0, J_2 = 2.4, 1H, indole-6H), 3.764 (s, 3H, o-methyl), 2.646 (s, 3H, c-methyl). ^{13}C NMR (150 MHz, d_6-DMSO): δ 184.1, 155.5, 148.6, 130.0, 126.4, 113.7, 112.1, 111.8, 102.3, 55.2, 11.5. Melting point: 188−192 °C (published:[54] 191−194 °C). TLC (ethyl acetate:hexane 4:1) R_f = 0.37. Elemental analysis calculated for $C_{11}H_{11}NO_2$: C, 69.83; H, 5.86; N, 7.40. Found: C, 69.65; H, 5.95; N, 7.25.

*trans-3-(5-Methoxy-2-methyl-1H-indol-3-yl)-1-(4-pyridinyl)-2-propen-1-one (**19**).* To a dried 250 mL two-neck round-bottom flask under argon, 2-methyl-5-methoxy-1*H*-indole-3-carboxaldehyde (1.51 g, 7.98 mmol) was dissolved in anhydrous MeOH (30 mL). 4-Acetyl-pyridine (1.32 mL, 11.97 mmol, 1.5 equiv) and piperidine (0.788 mL, 7.98 mmol) were added, and the reaction was stirred under reflux. An orange solid gradually precipitated, and this was isolated by filtration, rinsed with chilled MeOH, and dried under vacuum, yielding 2.08 g of orange solid (89%). ^{1}H NMR (600 MHz, d_6-DMSO): δ 11.909 (s, 1H, N−H), 8.812−8.802 (dd, J_1 = 4.2, J_2 = 1.8, 2H, pyr-2,6H), 8.097−8.072 (d, J = 15.0, 1H, C═CH), 7.947−7.937(dd, J_1 = 4.2, J_2 = 1.8, 2H, pyr-3,5H), 7.434−7.430 (d, J = 2.4, 1H, indole-4H), 7.374−7.349 (d, J = 15.0, 1H, C═CH), 7.315−7.301 (d, J = 8.4, 1H, indole-7H), 6.851−6.833 (dd, J_1 = 8.4, J_2 = 2.4, 1H, indole-6H), 3.860 (s, 3H, o-methyl), 2.572 (s, 3H, c-methyl). ^{13}C NMR (150 MHz, d_6-DMSO): δ 188.1, 155.2, 150.6, 145.8, 145.1, 136.6, 131.0, 126.6, 121.5, 112.8, 112.3, 110.9, 109.3, 103.5, 55.6, 12.2. Melting point: 252−256 °C. TLC (ethyl acetate:hexane 4:1) R_f = 0.16. Elemental analysis calculated for $C_{18}H_{16}N_2O_2$: C, 73.95; H, 5.52; N, 9.58. Found: C, 73.76; H, 5.46; N, 9.47.

*trans-3-(5-Methoxy-1-methyl-indol-3-yl)-1-(4-pyridinyl)-2-propen-1-one (**20**).* *N*,*N*-DMF (3 mL) was added to a dried 100 mL two-neck round-bottom flask under argon containing NaH (21 mg, 0.52 mmol, 60% in mineral oil, 1.2 equiv, unwashed). After this was stirred for 5 min, the starting material (120 mg, 0.43 mmol) dissolved in DMF (1 mL) was added slowly and stirred for 5 min until a homogeneous red solution was formed. Methyl iodide (40 μL, 0.65 mmol, 1.5 equiv) was added slowly. After 2 h, saturated NH_4Cl (20 mL) and H_2O (20 mL) were added; this was extracted with ethyl acetate (3 × 30 mL), dried with Na_2SO_4, filtered, and concentrated. The crude product was purified by column chromatography (methylene chloride:methanol 95:5), providing 103 mg (82%) of solid. NMR: ^{1}H NMR (400 MHz, d_6-DMSO): δ 8.821−8.806 (dd, J_1 = 4.4, J_2 = 1.6, 2H, pyr-2,6H), 8.143 (s, 1H, indole-2H), 8.081−8.042 (d, J = 15.6, 1H, C═CH), 7.950−7.935 (dd, J_1 = 4.4, J_2 = 1.6, 2H, pyr-3,5H), 7.517−7.473 (m, 3H, C═CH, indole-4,7H), 6.971−6.942 (dd, J_1 = 9.2, J_2 = 2.4, 1H, indole-6H), 3.875 (s, 3H, o-methyl), 3.838 (s, 3H, n-methyl). ^{13}C NMR (100 MHz, d_6-DMSO): δ 188.2, 155.5, 150.6, 144.9, 140.2, 137.3, 133.1, 126.5, 121.5, 114.2, 112.3, 111.9, 111.5, 102.9, 55.7, 33.4. Melting point: 178−182 °C. TLC (in methylene chloride:methanol 95:5) R_f = 0.35. Elemental analysis calculated for $C_{18}H_{16}N_2O_2\cdot0.1H_2O$: C, 73.50; H, 5.55; N, 9.52. Found: C, 73.34; H, 5.77; N, 9.25.

*trans-3-(5-Hydroxy-1H-indol-3-yl)-1-(4-pyridinyl)-2-propen-1-one (**21**).* In a dried 250 mL two-neck round-bottom flask under argon, **19** (500 mg, 1.71 mmol) was partially dissolved in anhydrous CH_2Cl_2 (35 mL) and placed at −78 °C. BBr_3 (17 mL, 1.0 M in CH_2Cl_2, 17 mmol) was added dropwise via an addition funnel under argon. After addition, the reaction was warmed to room temperature, and stirring was continued for 1 h. Ice water (50 mL) was added, followed by 1 N NaOH until the pH ≈ 12 (~60 mL). The CH_2Cl_2 was further extracted with 1 N NaOH (3 × 20 mL). The basic extracts were neutralized with 8 N HCl to a neutral pH (~8 mL), upon which the product precipitated. The precipitate was filtered and dried under vacuum, providing 454 mg (95%) of a yellow solid. NMR: ^{1}H NMR (600 MHz, d_6-DMSO): δ 11.833 (s, 1H, N−H), 9.072 (s, 1H, O−H), 8.818 (s, 2H, pyr-2,6H), 8.064−8.039 (d, J = 15.0, 1H, C═CH), 7.897 (s, 2H, pyr-3,5H), 7.342 (s, 1H, indole-4H), 7.282−7.257 (d, J = 15.0, 1H, C═CH), 7.209−7.195 (d, J = 8.4, 1H, indole-7H), 6.687−6.674 (d, J = 7.8, 1H, indole-6H), 2.542 (s, 3H, methyl). ^{13}C NMR (150 MHz, d_6-DMSO): δ 187.7, 153.0, 150.7, 145.9, 145.4, 140.0, 130.2, 126.8, 121.3, 112.2, 112.0, 111.6, 109.1, 105.2, 12.0. Melting point: 296−299 °C. TLC (in ethyl acetate:hexane 4:1) R_f = 0.19. Elemental analysis calculated for $C_{17}H_{14}N_2O_2\cdot0.1CH_2Cl_2$: C, 71.55; H, 4.99; N, 9.79. Found: C, 71.89; H, 5.02; N, 9.67.

*2-Methyl-1H-indol-5-ol (**22**).*[55] A dried 250 mL two-neck round-bottom flask was charged with 2-methyl-5-methoxyindole (1.00 g, 6.20 mmol) and purged with argon, and CH_2Cl_2 (30 mL) was added and stirred vigorously until the indole was dissolved. After the reaction was placed at −78 °C, BBr_3 (37.2 mL, 1.0 M in CH_2Cl_2, 37.2 mmol, 6 equiv) was added dropwise via an addition funnel under argon. After addition, the reaction was allowed to slowly warm to room temperature. Thirty minutes after the cooling bath was removed, the reaction was poured into ice water (~50 mL) and saturated $NaHCO_3$ (50 mL), to a neutral pH. This was extracted with CH_2Cl_2 (3 × 50 mL); the aqueous phase retained a yellow color and was acidified to pH ~3 (with 5 N HCl) and extracted with ethyl acetate (2 × 50 mL). The combined organic extracts were washed with brine, dried with Na_2SO_4, filtered, and concentrated to a brown oil. After it was dried under vacuum for 6 h, 845 mg of a pure brown solid was isolated (93%, 147.17 MW). ^{1}H NMR (600 MHz, d_6-DMSO): δ 10.538 (s, 1H, N−H), 8.476 (s, 1H, O−H), 7.028−7.014 (d, J = 8.4, 1H, indole-7H), 6.701−6.698 (d, J = 1.8, 1H, indole-4H), 6.487−6.468 (dd, J_1 = 9.0, J_2 = 2.4, 1H, indole-6H), 5.906 (s, 1H, indole-3H), 2.305 (s, 3H, methyl). ^{13}C NMR (150 MHz, d_6-DMSO): δ 150.4, 135.8, 130.6, 129.4, 110.6, 109.8, 103.3, 98.5, 13.5. Melting point: 131−134 °C (published:[55] 134 °C). TLC (in 1:1 ethyl acetate:hexanes) R_f = 0.28. Elemental analysis calculated for C_9H_8NO: C, 73.45; H, 6.16; N, 9.52. Found: C, 73.09; H, 6.29; N, 9.28.

*5-(4-Methylbenzoate)methoxy-2-methyl-1H-indole (**23**).* In a 250 mL round-bottom flask, 2-methyl-1*H*-indole-5-ol (670 mg, 4.55 mmol) was partially dissolved in CH_2Cl_2 (50 mL). Tetra-*n*-butylammonium bromide (808 mg, 2.5 mmol) was added, followed

by NaOH (50 mL of a 5 N solution, 250 mmol) and methyl 4-(bromomethyl)benzoate (1.15 g, 5.01 mmol, 1.1 equiv). After 8 h, the organic layer was removed, and the aqueous phase was extracted with CH_2Cl_2 (1 × 30 mL). The combined extracts were washed with brine, dried with Na_2SO_4, filtered, and concentrated to an oil. Purification by column chromatography (1:3 ethyl acetate:hexane) provided 839 mg of pure product (63%, 295.33 MW) [followed by the 3,5-doubly alkylated product (115 mg, 5%)]. ^{1}H NMR (600 MHz, d_6-DMSO): δ 10.755 (s, 1H, N−H), 7.980−7.966 (d, J = 8.4, 2H, phenyl-3,5H), 7.602−7.588 (d, J = 8.4, 2H, phenyl-2,6H), 7.150−7.136 (d, J = 8.4, 1H, indole-7H), 6.982−6.978 (d, J = 2.4, 1H, indole-4H) 6.717−6.699 (dd, J_1 = 8.4, J_2 = 2.4, 1H, indole-6H), 6.005 (s, 1H, indole-3H), 5.157 (s, 2H, methylene), 3.849 (s, 3H, o-methyl), 2.331 (s, 3H, c-methyl). ^{13}C NMR (150 MHz, d_6-DMSO): δ 166.1, 151.9, 143.6, 136.3, 131.4, 129.3, 129.0, 128.7, 127.4, 111.0, 110.1, 102.8, 99.0, 69.0, 52.1, 13.4. Melting point: 151−154 °C. TLC (in 1:1 ethyl acetate:hexanes) R_f = 0.49 (doubly alkylated product R_f = 0.42). Elemental analysis calculated for $C_{19}H_{17}NO_3$: C, 73.20; H, 5.80; N, 4.74. Found: C, 73.02; H, 5.82; N, 4.55.

*5-(4-Methylbenzoate)methoxy-2-methyl-1H-indole-3-carboxaldehyde (**24**).* To a dried two-neck 250 mL round-bottom flask under argon, $POCl_3$ (325 μL, 3.5 mmol) was added to *N*,*N*-DMF (8 mL) at 0 °C. After this was stirred for 5 min, **23** (320 mg, 1.08 mmol) dissolved in DMF (4 mL) was added dropwise. The yellow solution was slowly warmed to room temperature, and after 1 h, saturated $NaHCO_3$ was added (50 mL), producing a white precipitate, followed by 1 N NaOH (20 mL) to complete precipitation (direct workup with NaOH resulted in roughly 1:1 mixture of ester product to ester-hydrolyzed analogue). The solid was filtered, rinsed with cold H_2O, and dried under vacuum, yielding 315 mg of white solid (90%). ^{1}H NMR (600 MHz, d_6-DMSO): δ 11.902 (s, 1H, N−H), 10.000 (s, 1H, CHO), 7.991−7.977 (d, J = 8.4, 2H, phenyl-3,5H), 7.664−7.660 (d, J = 2.4, 1H, indole-4H), 7.633−7.619 (d, J = 8.4, 2H, phenyl-2,6H), 7.304−7.290 (d, J = 8.4, 1H, indole-7H), 6.906−6.887 (dd, J_1 = 9.0, J_2 = 2.4, 1H, indole-6H), 5.211 (s, 2H, methylene), 3.854 (s, 3H, o-methyl), 2.646 (s, 3H, c-methyl). ^{13}C NMR (150 MHz, d_6-DMSO): δ 184.0, 166.1, 154.3, 148.7, 143.2, 130.4, 129.3, 128.8, 127.4, 126.4, 113.6, 112.3, 112.2, 104.0, 69.0, 52.1, 11.5. Melting point: 224−227 °C. TLC: (in ethyl acetate:hexanes 4:1) R_f = 0.35. Elemental analysis calculated for $C_{19}H_{17}NO_4$: C, 70.58; H, 5.30; N, 4.33. Found: C, 70.45; H, 5.41; N, 4.51.

*5-(4-Benzoate)methoxy-2-methyl-1H-indole-3-carboxaldehyde (**25**).* To a dried two-neck 250 mL round-bottom flask under argon, $POCl_3$ (565 μL, 6.1 mmol) was added to *N*,*N*-DMF (12 mL) at 0 °C. After this was stirred for 5 min, **23** (600 mg, 2.03 mmol) dissolved in DMF (9 mL) was added dropwise. The yellow solution was slowly warmed to room temperature. After 1 h, the reaction was cooled to 0 °C, and 5 N NaOH (90 mL) was added. After this was stirred for 30 min, 5 N HCl (95 mL) was added to precipitate the product, which was filtered and dried overnight under vacuum, yielding 626 mg (99%) of white solid. ^{1}H NMR (600 MHz, d_6-DMSO): δ 11.944 (s, 1H, N−H), 10.001 (s, 1H, CHO), 7.961−7.947 (d, J = 8.4, 2H, phenyl-3,5H), 7.664−7.660 (d, J = 2.4, 1H, indole-4H), 7.590−7.576 (d, J = 8.4, 2H, phenyl-2,6H), 7.304−7.290 (d, J = 8.4, 1H, indole-7H), 6.902−6.884 (dd, J_1 = 8.4, J_2 = 2.4, 1H, indole-6H), 5.194 (s, 2H, methylene), 2.647 (s, 3H, methyl). ^{13}C NMR (150 MHz, d_6-DMSO): δ 184.0, 167.3, 154.4, 148.8, 142.5, 130.4, 129.4, 127.3, 127.2, 126.4, 113.6, 112.3, 112.2, 104.0, 69.1, 11.5. Melting point: 267−270 °C. TLC: (in ethyl acetate:hexanes 4:1) R_f = 0.25.

*trans-3-[5-((4-Methylbenzoate)methoxy)-1H-indol-3-yl)]-1-(4-pyridinyl)-2-propen-1-one (**26**).* In a dried 100 mL two-neck round-bottom flask under argon, **24** (50 mg, 0.15 mmol) was partially dissolved in anhydrous methanol (2 mL). 4-Acetyl-pyridine (26 μL, 0.23 mmol) and piperidine (7 μL, 0.075 mmol) were added, and the reaction was refluxed. A yellow precipitate gradually formed, and after 24 h, the reaction was brought to room temperature, and the solid was isolated by filtration, rinsed with cold methanol, and dried under vacuum, yielding 36 mg. However, crude NMR showed 1:0.15 product:aldehyde. This mixture was dry loaded onto silica and purified by column chromatography (ethyl acetate:hexanes 2:1), providing 22 mg of pure product (34%). ^{1}H NMR (600 MHz, d_6-DMSO): δ 11.937 (s, 1H, N−H), 8.829−8.819 (d, J = 6.0, 2H, pyr-2,6H), 8.069−8.044 (d, J = 15.0, 1H, C═CH), 7.971−7.957 (d, J = 8.4, 2H, phenyl-3,5H), 7.905−7.896 (d, J = 5.4, 2H, pyr-3,5H), 7.662−7.649 (d, J = 7.8, 2H, phenyl-2,6H), 7.479−7.475 (d, J = 2.4, 1H, indole-4H), 7.326−7.312 (d, J = 8.4, 1H, indole-7H), 7.284−7.259 (d, J = 15.0, 1H, C═CH), 6.938−6.920 (dd, J_1 = 8.7, J_2 = 2.1, 1H, indole-6H), 5.358 (s, 2H, methylene), 3.838 (s, 3H, o-methyl), 2.561 (s, 3H, c-methyl). ^{13}C NMR (150 MHz, d_6-DMSO): δ 188.1, 166.0, 153.9, 150.6, 146.0, 145.1, 143.5, 139.5, 131.3, 129.3, 128.8, 127.4, 126.4, 121.4, 112.8, 112.4, 111.9, 109.3, 104.8, 69.2, 52.2, 12.1. Melting point: 236−239 °C. TLC (ethyl acetate:hexanes 4:1) R_f = 0.26. Elemental analysis calculated for $C_{26}H_{22}N_2O_4 \cdot 0.25C_4H_8O_2$: C, 72.31; H, 5.39; N, 6.25. Found: C, 72.62; H, 5.64; N, 5.95.

*trans-3-[5-((4-Carboxyphenyl)-methoxy)-1H-indol-3-yl)]-1-(4-pyridinyl)-2-propen-1-one (**27**).* In a dried 100 mL round-bottom flask under argon, **25** (200 mg, 0.65 mmol) was partially dissolved in anhydrous methanol (15 mL). 4-Acetyl-pyridine (107 μL, 0.97 mmol, 1.5 equiv) and piperidine (256 μL, 0.65 mmol) were added, and the reaction was refluxed. After 24 h, the solid precipitate was isolated by filtration, yielding 75 mg of product contaminated with aldehyde. Because of both solubility and poor filtration, plenty of product remained in the filtrate; thus, the filtrate was dry loaded onto silica and purified by column chromatography (methylene chloride:methanol 9:1), yielding 85 mg of purified acid product (21%). ^{1}H NMR (600 MHz, d_6-DMSO): δ 11.947 (s, 1H, N−H), 8.831−8.821 (dd, J_1 = 4.2, J_2 = 1.8, 2H, pyr-2,6H), 8.073−8.047 (d, J = 15.6, 1H, C═CH), 7.954−7.941 (d, J = 7.8, 2H, phenyl-3,5H), 7.904−7.894 (dd, J_1 = 4.2, J_2 = 1.8, 2H, pyr-3,5H), 7.630−7.616 (d, J = 8.4, 2H, phenyl-2,6H), 7.479−7.476 (d, J = 1.8, 1H, indole-4H), 7.326−7.312 (d, J = 8.4, 1H, indole-7H), 7.289−7.264 (d, J = 15.0, 1H, C═CH), 6.939−6.920 (dd, J_1 = 9.0, J_2 = 2.4, 1H, indole-6H), 5.349 (s, 2H, methylene), 2.562 (s, 3H, methyl). ^{13}C NMR (150 MHz, d_6-DMSO): δ 188.1, 167.3, 154.0, 150.6, 146.0, 145.1, 142.8, 139.6, 131.2, 130.3, 129.5, 127.2, 126.4, 121.4, 112.8, 112.4, 111.9, 109.3, 104.8, 69.3, 12.1. Melting point: 269−273 °C. TLC (methylene chloride:methanol 9:1) R_f = 0.41. Elemental analysis calculated for $C_{25}H_{20}N_2O_4 \cdot 0.25$ $CH_2Cl_2 \cdot 0.25CH_3OH$: C, 69.34; H, 4.91; N, 6.34. Found: C, 69.28; H, 5.22; N, 6.72.

*2-Methyl-5-benzoyl-indole-3-carboxaldehyde and 2-Methyl-6-benzoyl-indole-3-carboxaldehyde (**28** and **29**).* In a dried two-neck 250 mL round-bottom flask under argon, *N*,*N*-DMF (339 μL, 4.4 mmol) was added to 1,2-dichloroethane (8 mL). The reaction was cooled to 0 °C, and oxalyl chloride (377 μL, 4.4 mmol) dissolved in 1,2-DCE (8 mL) was slowly added, forming a white heterogeneous mixture. The mixture was allowed to warm to room temperature while stirring. After 15 min, the reaction was cooled to 0 °C, and 2-methylindole (577 mg, 4.0 mmol) dissolved in 1,2-DCE (8 mL) was slowly added, forming a dark red solution. After 1 h, $AlCl_3$ (1.96 g, 14.7 mmol) was added and stirred vigorously. Benzoyl chloride (510 μL, 4.4 mmol) dissolved in 1,2-DCE (4 mL) was slowly added, and the reaction was warmed to room temperature and stirred overnight. After 24 h, cold H_2O (50 mL) was added, followed by 5 N NaOH (10 mL), and the mixture was stirred. After 1 h, 5 N HCl (18 mL) was added, and this was extracted with methylene chloride (3 × 50 mL). The combined 1,2-DCE and methylene chloride extracts were combined, dried with Na_2SO_4, filtered, and concentrated. The crude product mixture was purified by column chromatography (ethyl acetate:hexanes 1:1 → 4:1), yielding 5-benzoyl product **28** (142 mg, 13%) and 6-benzoyl product **29** (429 mg, 41%) (1:3 regioselectivity for 5 vs 6 benzoylation).

*2-Methyl-5-benzoyl-indole-3-carboxaldehyde (**28**).* ^{1}H NMR (600 MHz, d_6-DMSO): δ 12.371 (s, 1H, N−H), 10.073 (s, 1H), CHO, 8.462 (s, 1H, indole-4H), 7.723−7.711 (m, 2H, phenyl-2,6H), 7.673−7.656 (m, 2H, indole-6H, phenyl-4H), 7.587−7.561 (t, J = 7.8, 2H, phenyl-3,5H), 7.553−7.539 (d, J = 8.4, 1H, indole-7H), 2.728 (s, 3H, methyl). ^{13}C NMR (150 MHz, d_6-DMSO): δ 196.1, 184.8, 150.8, 138.3, 138.0, 132.1, 130.9, 129.5, 128.5, 124.9, 124.7, 123.4, 114.4, 111.6, 11.6. 1-D NOE: irradiation of peak at δ 12.371 (N−H): NOE signal enhancement seen at δ 7.549 (C−H) and 2.728 (CH_3). The H

peak at 7.549 has *ortho* coupling (J = 8.4), proving the benzoyl group inserted at the 5-position, not 6. Separately, irradiation of peak at δ 7.540 (C−H with *ortho* coupling): NOE signal enhancement seen at δ 12.370 (N−H), again proving the proximity of N−H to an ortho-coupled C_7−H; signal enhancement also seen at δ 7.66 for C_6−H (the benzoyl 2H triplet peak at δ 7.574 was also irradiated by proximity, thus signal enhancement was seen for the other benzoyl C−H peaks at δ 7.72 and δ 7.67). Melting point: 227−230 °C. TLC (ethyl acetate:hexanes 4:1) R_f = 0.32. Elemental analysis calculated for $C_{17}H_{13}NO_2 \cdot 0.2C_4H_8O_2$ (trace ethyl acetate): C, 76.11; H, 5.24; N, 4.99. Found: C, 75.74; H, 4.94; N, 5.06.

*2-Methyl-6-benzoyl-indole-3-carboxaldehyde (**29**).* ^{1}H NMR (600 MHz, d_6-DMSO): δ 12.323 (s, 1H, N−H), 10.116 (s, 1H, CHO), 8.173−8.159 (d, J = 8.4, 1H, indole-4H), 7.776−7.774 (d, J = 1.2, 1H, indole-7H), 7.741−7.729 (m, 2H, phenyl-2,6H), 7.683−7.659 (t, J = 7.2, 1H, phenyl-4H), 7.627−7.611 (dd, J_1 = 7.8, J_2 = 1.8, 1H, indole-5H), 7.583−7.558 (t, J = 7.5, 2H, phenyl-3,5H), 2.744 (s, 3H, methyl). ^{13}C NMR (150 MHz, d_6-DMSO): δ 196.3, 185.4, 152.2, 138.7, 135.3, 132.8, 131.8, 130.1, 129.8, 129.1, 124.4, 120.3, 114.7, 114.4, 12.5. 1-D NOE: irradiation of peak at δ 12.323 (N−H): NOE signal enhancement seen at δ 7.775 (C−H with *meta* coupling, thus proving benzoyl addition to position 6 of indole) and δ 2.744 (CH_3). Separately, irradiation of the peak at δ 7.775 (C−H with *meta* coupling: J = 1.2) led to signal enhancement at δ 12.323 (N−H peak), thus proving proximity of meta-coupled C−H to N−H (the benzoyl 2,6 2H peak at 7.73 was also irradiated by proximity, leading to signal enhancement of benzoyl 3,5 2H peak at δ 7.57). Melting point: 192−196 °C. TLC (ethyl acetate:hexanes 4:1) R_f = 0.40. Elemental analysis calculated for $C_{17}H_{13}NO_2$: C, 77.55; H, 4.98; N, 5.32. Found: C, 77.28; H, 4.97; N, 5.15.

*trans-3-(5-Benzoyl-2-methyl-1H-indol-3-yl)-1-(4-pyridinyl)-2-propen-1-one (**30**).* In a dried 100 mL round-bottom flask under argon, **28** (50 mg, 0.19 mmol) was dissolved in anhydrous methanol (3 mL). 4-Acetyl-pyridine (21 μL, 0.19 mmol) and piperidine (4 μL, 0.04 mmol) were added, and the reaction was refluxed. After 12 h, 0.3 equiv of 4-acetyl-pyridine (6.3 μL, 0.06 mmol) was added. After a total of 24 h of reaction time, the reaction was cooled, and the precipitate was isolated by filtration and rinsed with cold methanol, providing 37 mg of yellow solid. A crude ^{1}H NMR showed a 1:3.5 ratio of product to aldehyde. The filtrate was concentrated and added to the product/aldehyde mixture, and 0.8 equiv of both 4-acetyl-pyridine (17 μL, 0.15 mmol) and piperidine (15 μL, 0.15 mmol) were added to the reaction. This was refluxed for another 24 h, after which the reaction was cooled, filtered, and rinsed with cold methanol, providing 9 mg (13%) of pure, yellow product. ^{1}H NMR (600 MHz, d_6-DMSO): δ 12.397 (s, 1H, N−H), 8.815−8.805 (m, 2H, pyr-2.6H), 8.321 (s, 1H, indole-4H), 8.081−8.056 (d, J = 15.0, 1H, C═CH), 7.820−7.808 (d, J = 7.2, 2H, phenyl-2,6H), 7.761−7.728 (m, 4H, phenyl-4H, indole-6H, pyr-3,5H), 7.644−7.619 (t, J = 7.5, 2H, phenyl-3,5H), 7.587−7.573 (d, J = 8.4, 1H, indole-7H), 7.347−7.321 (d, J = 15.6, 1H, C═CH), 2.639 (s, 3H, methyl). ^{13}C NMR (150 MHz, d_6-DMSO): δ 195.7, 187.9, 150.6, 146.9, 144.7, 138.8, 138.5, 138.4, 131.9, 130.1, 129.4, 128.4, 125.2, 123.9, 123.6, 121.1, 114.6, 111.9, 110.1, 12.1. Melting point: 258−262 °C. TLC (ethyl acetate:hexanes 4:1) R_f = 0.24. Elemental analysis calculated for $C_{24}H_{18}N_2O_2 \cdot 0.65H_2O$: C, 76.24; H, 5.14; N, 7.41; C, 75.96; H, 4.75; N, 7.16.

*trans-3-(6-Benzoyl-2-methyl-1H-indol-3-yl)-1-(4-pyridinyl)-2-propen-1-one (**31**).* In a dried 100 mL round-bottom flask under argon, **29** (50 mg, 0.19 mmol) was dissolved in anhydrous methanol (3 mL). 4-Acetyl-pyridine (21 μL, 0.19 mmol) and piperidine (19 μL, 0.19 mmol) were added, and the reaction was refluxed. After 24 h, the reaction was cooled, filtered, and rinsed with cold hexanes and dried under vacuum, yielding 52 mg (74%) of pure yellow solid. ^{1}H NMR (600 MHz, d_6-DMSO): δ 12.350 (s, 1H, N−H), 8.832−8.222 (d, J = 6.0, 2H, pyr-2,6H), 8.255−8.241 (d, J = 8.4, 1H, indole-4H), 8.125−8.099 (d, J = 15.6, 1H, C═CH), 8.008−7.999 (d, J = 5.4, 2H, pyr-3,5H), 7.801 (s, 1H, indole-7H), 7.766−7.754 (d, J = 7.2, 2 H, phenyl-2,6H), 7.683−7.642 (m, 2H, phenyl-4H, indole-5H), 7.585−7.563 (m, 3H, C═CH, phenyl-3,5H), 2.659 (s, 3H, methyl). ^{13}C NMR (150 MHz, d_6-DMSO): δ 195.5, 188.2, 150.6, 148.5, 144.6, 138.7, 138.2, 135.4, 132.0, 130.6, 129.4, 129.2, 128.4, 123.1, 121.5, 119.9, 114.5, 114.1, 109.6, 12.3. Melting point: 267−270 °C. TLC (ethyl acetate:hexanes 4:1) R_f = 0.29. Elemental analysis calculated for $C_{24}H_{18}N_2O_2 \cdot 0.05H_2O$: C, 78.48; H, 4.97; N, 7.63. Found: C, 78.08; H, 5.01; N, 7.50.

*2-Methyl-5-nitro-1H-indole (**32**).*[26] In a 250 mL round-bottom flask, 2.62 g of 2-methyl-indole (20 mmol) was dissolved in 20 mL of H_2SO_4 after vigorous stirring. In a separate flask, 1.87 g of $NaNO_3$ (1.1×, 22 mmol, 84.99 MW) was dissolved in 20 mL of H_2SO_4, also after vigorous stirring, and added dropwise via addition funnel to the indole. After addition, the reaction was stirred for another 10 min and then poured into 400 mL of ice water, precipitating a yellow product. The product was isolated via filtration and washed with cold water. After 12 h of drying under vacuum, 3.35 g of yellow product was isolated (95%). ^{1}H NMR (600 MHz, d_6-DMSO): δ 11.703 (s, 1H, N−H), 8.4003−8.400 (d, J = 1.8, 1H, indole-4H), 7.916−7.898 (dd, J_1 = 9.0, J_2 = 1.8, 1H, indole-6H), 7.422−7.407 (d, 1H, J = 9.0, 1H, indole-7H), 6.408 (s, 1H, indole-3H), 2.419 (s, 1H, methyl). ^{13}C NMR (150 MHz, d_6-DMSO): δ 140.5, 140.0, 139.4, 128.0, 115.9, 115.7, 110.7, 101.6, 13.4. 1-D NOE: irradiation of peak at δ 7.422−7.407 (C_7−H): NOE signal enhancement seen at δ 11.690 (N−H) and 7.916−7.897 (C_6−H). Irradiation of peak at δ 11.690 (N−H): NOE signal enhancement seen at δ 7.422−7.407 (C_7−H) and 2.419 (C_2−CH_3) (NOE observed between the C−H proton with *ortho* coupling and N−H proton, thus proving NO_2 inserted at indole C-5 vs C-6). Melting point: 166−169 °C (published:[26] 176−176.5 °C). TLC (in 1:1 ethyl acetate:hexanes) R_f = 0.38. Elemental analysis calculated for $C_9H_8N_2O_2$: C, 61.36; H, 4.58; N, 15.90. Found: C, 61.54; H, 4.63; N, 15.89.

*2-Methyl-5-amino-1H-indole (**33**).*[26] Compound **32** (1.00 g, 5.68 mmol) was dissolved in 75 mL of ethanol. 10% Pd/C was added (200 mg), and the mixture was subjected to H_2 (38 psi) using a Parr hydrogenator for 3.5 h. The mixture was filtered over Celite, which was washed with methanol. After concentration and drying under vacuum, 801 mg of a brown powder (97%) was isolated. ^{1}H NMR (600 MHz, d_6-DMSO): δ 10.370 (s, 1H, N−H), 6.943−6.929 (d, J = 8.4, 1H, indole-7H), 6.552−6.549 (d, J = 1.8, 1H, indole-4H), 6.373−6.355 (dd, J_1 = 8.4, J_2 = 2.4, 1H), 5.815 (s, 1H, indole-6H), 4.436 (bs, 2H, NH_2), 2.288 (s, 3H, methyl). ^{13}C NMR (150 MHz, d_6-DMSO): δ 140.8, 135.0, 129.9, 129.6, 110.5, 110.3, 102.9, 98.0, 13.5. Melting point: 147−150 °C (published:[26] 157−159 °C). TLC (in 3:1 ethyl acetate:hexanes) R_f = 0.30; (in 1:1 ethyl acetate:hexanes) R_f = 0.16. Elemental analysis calculated for $C_9H_{10}N_2 \cdot 0.05C_2H_6O$: C, 73.61; H, 6.99; N, 18.87. Found: C, 73.48; H, 6.77; N, 18.81.

*2-Methyl-5-azido-1H-indole (**34**).* In an oven-dried, 250 mL round-bottom flask flushed with argon, **33** (400 mg, 2.74 mmol, 146.19 MW) was dissolved in 90% AcOH (20 mL). After complete solvation, the reaction was placed at 0 °C and protected from light with foil. $NaNO_2$ (1.1×, 3.01 mmol, 208 mg, 69.00 MW) dissolved in cold H_2O (2 mL) was added dropwise and stirred for 10 min. NaN_3 (1.1×, 3.01 mmol, 196 mg, 65.01 MW) dissolved in cold H_2O (2 mL) was added dropwise. After 1 h, the reaction was poured into water (40 mL), which was extracted 3 times with CH_2Cl_2 (40 mL each). The extracts were washed with sodium bicarbonate and brine (100 mL each), dried with sodium sulfate, filtered, and concentrated. Purification by silica flash chromatography (100% CH_2Cl_2) yielded the azide as a light brown solid (310 mg, 66%). ^{1}H NMR (600 MHz, d_6-DMSO): δ 11.025 (s, 1H, N−H), 7.295−7.281 (d, J = 8.4, 1H, indole-7H), 7.131−7.127 (d, J = 2.4, 1H, indole-4H), 6.737−6.719 (dd, J_1 = 8.4, J_2 = 2.4, 1H, indole-6H), 6.108−6.106 (d, J = 1.2, 1H, indole-3H), 2.369 (s, 1H, methyl). ^{13}C NMR (150 MHz, d_6-DMSO): δ 137.5, 133.9, 130.0, 129.5, 111.7, 111.6, 108.5, 99.0, 13.4. Melting point: 57−60 °C. TLC (in 1:1 ethyl acetate:hexanes) R_f = 0.56. IR (film): 3409 cm^{-1}, 2111 (aryl-azide). Elemental analysis calculated for $C_9H_8N_4$: C, 62.78; H, 4.68; N, 32.54. Found: C, 62.95; H, 4.68; N, 32.53.

*2-Methyl-3-carboxaldehyde-5-azido-1H-indole (**35**).* In an oven-dried, 100 mL round-bottom flask purged with argon, $POCl_3$ (1.5×, 3.14 mmol, 291 μL) was added to anhydrous DMF (2.0 mL) at 0 °C. Compound **34** (dissolved in DMF, 2 mL) was added dropwise. The stirred reaction was slowly warmed to room temperature (RT). NaOH

(1 N, 25 mL) and water (25 mL) were added, forming a precipitate that was filtered and rinsed with cold water. The resulting white solid was dried under vacuum, affording 369 mg (88%). ^{1}H NMR (600 MHz, d_6-DMSO): δ 12.078 (s, 1H, N−H), 10.031 (s, 1H, CHO), 7.754−7.751 (d, J = 1.8, 1H, indole-4H), 7.423−7.409 (d, J = 8.4, 1H, indole-7H), 6.913−6.896 (dd, J_1 = 8.4, J_2 = 1.8, 1H, indole-6H), 2.676 (s, 3H, methyl). ^{13}C NMR (150 MHz, d_6-DMSO): δ 184.3, 149.7, 133.4, 133.0, 126.6, 114.4, 113.4, 112.8, 109.4, 11.5. Melting point: degradation ca. 150 °C. TLC (in 1:1 ethyl acetate:hexanes) R_f = 0.19. Elemental analysis calculated for $C_{10}H_8N_4O$: C, 59.99; H, 4.03; N, 27.99. Found: C, 60.03; H, 4.07; N, 27.96.

*trans-3-(5-Azido-2-methyl-1H-indol-3-yl)-1-(4-pyridinyl)-2-propen-1-one (**36**).* In a dried, 100 mL round-bottom flask under argon and protected from light, **35** (80 mg, 0.40 mmol) was partially dissolved in anhydrous methanol (5 mL). 4-Acetyl-pyridine (1.5 equiv, 66 μL, 0.60 mmol) and piperidine (40 μL, 0.40 mmol) were added, and the reaction was stirred at 40 °C. After 24 h, the reaction was cooled to RT, and the yellow precipitate was isolated via filtration and rinsed with cold methanol. A crude ^{1}H NMR of this product showed a ca. 1:3 ratio of product to the indole starting material. This crude product was redissolved in anhydrous methanol (5 mL) along with the concentrated filtrate, and another equivalent of 4-acetyl-pyridine (44 μL, 2.5 equiv total) and 5 equiv of piperidine (200 μL, 6 equiv total) were added. The stirred reaction was heated at 40 °C. After 12 h, a yellow precipitate was filtered and rinsed with cold methanol and dried under vacuum, affording 47 mg (39%) of pure product. ^{1}H NMR (600 MHz, d_6-DMSO): δ 12.105 (s, 1H, N−H), 8.816−8.806 (dd, J_1 = 4.8, J_2 = 1.8, 2H, pyr-2,6H), 8.066−8.041 (d, J = 15, 1H, C═CH), 7.956−7.945 (dd, J_1 = 4.8, J_2 = 1.8, 2H, pyr-3,5H), 7.661−7.657 (d, J = 2.4, 1H, indole-4H), 7.455−7.441 (d, J = 8.4, 1H, indole-7H), 7.401−7.375 (d, J = 15.6, 1H, C═CH), 7.001−6.984 (dd, J_1 = 8.4, J_2 = 1.8, indole-6H), 2.587 (s, 3H, methyl). ^{13}C NMR (150 MHz, d_6-DMSO): δ 188.2, 150.6, 146.5, 144.9, 139.0, 133.9, 132.9, 126.8, 121.5, 113.9, 113.8, 113.0, 110.3, 109.2, 12.2. Melting point: decomposes ca. 190 °C. TLC (in 4:1 ethyl acetate:hexanes) R_f = 0.21. Elemental analysis calculated for $C_{17}H_{13}N_5O$: C, 67.32; H, 4.32; N, 23.09. Found: C, 67.37; H, 4.33; N, 23.12.

*2-Methyl-5-methoxy-6-nitro-1H-indole (**37**).* In a 100 mL round-bottom flask, 2-methyl-5-methoxyindole (370 mg, 2.30 mmol) was dissolved in H_2SO_4 (4 mL) after vigorous stirring, then placed at 0 °C. In a separate flask, 1.87 g of $NaNO_3$ (214 mg, 2.52 mmol) was dissolved in H_2SO_4 (4 mL), also after vigorous stirring, chilled to 0 °C, and added dropwise to the indole. After addition, the reaction was stirred for another 10 min and then poured into ice−water (200 mL), precipitating a yellow product, which was extracted with ethyl acetate (3 × 100 mL). Extracts were washed with saturated $NaHCO_3$ and brine, dried with Na_2SO_4, filtered, and concentrated. Purification by column chromatography (ethyl acetate:hexane 2:3 → 3:2) yielded 296 mg of pure product (62%) (followed by 73 mg of 4-nitrated product, 15%; 4:1 regioselectivity). ^{1}H NMR (600 MHz, $CDCl_3$): δ 8.350 (s, 1H, N−H), 7.983 (s, 1H, indole-7H), 7.066 (s, 1H, indole-4H), 6.211 (s, 1H, indole-3H), 3.958 (s, 3H, o-methyl), 2.477 (s, 3H, c-methyl). ^{13}C NMR (150 MHz, $CDCl_3$): δ 148.7, 142.8, 134.7, 134.2, 129.1, 109.2, 102.7, 101.3, 57.1, 14.2. Melting point: 134−138 °C. TLC (in 1:1 ethyl acetate:hexanes) R_f = 0.37 (4-nitro product R_f = 0.25). Elemental analysis calculated for $C_{10}H_{10}N_2O_3{\cdot}0.1C_6H_{14}$: C, 59.27; H, 5.35; N, 13.04. Found: C, 59.33; H, 5.10; N, 12.98.

*2-Methyl-5-methoxy-6-amino-1H-indole (**38**).* In a hydrogenation flask, **37** (270 mg, 1.31 mmol) was dissolved in 100% EtOH (35 mL), and 10% Pd/C (40 mg) was added. The mixture was hydrogenated on a Parr hydrogenator at 40 psi for 45 min. The red-pink solution was filtered over Celite and rinsed with MeOH, concentrated, and dried under vacuum, yielding 230 mg of pure product (99%). ^{1}H NMR (400 MHz, $CDCl_3$): δ 7.516 (s, 1H, N−H), 6.907 (s, 1H), 6.607 (s, 1H), 6.052 (s, 1H, indole-3H), 3.873 (s, 3H, o-methyl), 3.733 (bs, 2H, NH_2), 2.365 (s, 3H, c-methyl). ^{13}C NMR (150 MHz, d_6-DMSO): δ 142.8, 132.9, 131.5, 131.4, 119.5, 100.5, 98.7, 95.7, 55.6, 13.5 Melting point: 144−148 °C. TLC (in 3:1 ethyl acetate:hexanes) R_f = 0.33. Elemental analysis calculated for $C_{10}H_{10}N_2O_3{\cdot}0.1C_6H_{14}$: C, 59.27; H, 5.35; N, 13.04. Found: C, 59.33; H, 5.10; N, 12.98.

*2-Methyl-5-methoxy-6-azido-1H-indole (**39**).* In a dried, 100 mL round-bottom flask under argon, **38** (227 mg, 1.29 mmol) was dissolved in 90% AcOH (10 mL) and placed at 0 °C. The flask was covered with foil, and the reaction was conducted in low light. $NaNO_2$ (98 mg, 1.43 mmol, 1.1 equiv) dissolved in H_2O (1 mL) was added dropwise, and the mixture was stirred for 10 min. NaN_3 (92 mg, 1.43 mmol, 1.1 equiv) dissolved in H_2O (1 mL) was added dropwise. After 45 min, the mixture was slowly poured into H_2O (25 mL) and saturated K_2CO_3 (19 mL) to form a neutral pH. This was extracted with ethyl acetate (4 × 50 mL), washed with brine, dried with Na_2SO_4, filtered, and concentrated. The crude product was purified by column chromatography (ethyl acetate:hexanes 1:4), yielding 139 mg of pure oil (53%). ^{1}H NMR (600 MHz, $CDCl_3$): δ 7.782 (s, 1H, N−H), 7.007 (s, 1H), 6.883 (s, 1H), 6.145 (s, 1H, indole-3H), 3.890 (s, 3H, o-methyl), 2.388 (s, 3H, c-methyl). ^{13}C NMR (150 MHz, $CDCl_3$): δ 147.0, 136.1, 130.7, 126.5, 123.1, 102.4, 102.0, 100.4, 56.5, 13.7. TLC (in 1:1 ethyl acetate:hexanes) R_f = 0.60.

*2-Methyl-3-carboxaldehyde-5-methoxy-6-azido-1H-indole (**40**).* In an oven-dried, 100 mL round-bottom flask, purged with argon and protected from light with foil, $POCl_3$ (84 μL, 0.90 mmol, 1.5 equiv) was added to anhydrous DMF (1.0 mL) at 0 °C and stirred for 5 min. Next, **39** (dissolved in DMF, 1 mL) was added dropwise. The stirred reaction was slowly warmed to RT. NaOH (1 N, 10 mL) and water (10 mL) were added, and this was extracted with CH_2Cl_2 (3 × 20 mL). Extracts were washed with brine, dried with Na_2SO_4, filtered, concentrated, and dried overnight under vacuum, producing 95 mg of pure product (69%). ^{1}H NMR (600 MHz, d_6-DMSO): δ 11.865 (s, 1H, N−H), 10.004 (s, 1H, CHO), 7.645 (s, 1H, indole-4H), 7.032 (s, 1H, indole-7H), 3.857 (s, 3H, o-methyl), 2.645 (s, 3H, c-methyl). ^{13}C NMR (150 MHz, d_6-DMSO): δ 184.8, 149.5, 149.4, 130.3, 124.1, 124.0, 114.4, 104.2, 103.5, 56.9, 12.2. TLC (in 1:1 ethyl acetate:hexanes) R_f = 0.12.

*trans-3-(6-Azido-5-methoxy-2-methyl-1H-indol-3-yl)-1-(4-pyridinyl)-2-propen-1-one (**41**).* In a dried, 100 mL round-bottom flask under argon and protected from light, **40** (70 mg, 0.30 mmol) was partially dissolved in anhydrous methanol (5 mL). 4-Acetyl-pyridine (50 μL, 0.45 mmol, 1.5 equiv) and piperidine (148 μL, 1.5 mmol, 5 equiv) were added, and the reaction was stirred at 40 °C. After 7 h, the reaction was cooled to RT, and the precipitate was isolated via filtration and rinsed with cold methanol. A crude ^{1}H NMR of this product showed a mixture of aldehyde with trace product. This mixture was redissolved in the filtrate, more 4-acetyl-pyridine (165 μL, 5 equiv) and piperidine (148 μL, 5 equiv) were added, and the mixture was set to react at 40 °C. After 48 h, although starting materials are still seen on TLC, the crude reaction mixture was dry loaded onto silica and purified by column chromatography (ethyl acetate:hexane 3:1), eluting first the aldehyde, followed by the ketone, and finally the product as a yellow solid (39 mg, 39%). ^{1}H NMR (600 MHz, d_6-DMSO): δ 11.784 (s, 1H, N−H), 8.815−8.805 (dd, J_1 = 4.2, J_2 = 1.8, 2H, pyr-2,6H), 8.073−8.047 (d, J = 15.6, 1H, C═CH), 7.957−7.947 (dd, J_1 = 4.2, J_2 = 1.8, 2H, pyr-3,5H), 7.538 (s, 1H, indole-4H), 7.410−7.384 (d, J = 15.6, 1H, indole C═CH), 7.051 (s, 1H, indole-7H), 3.982 (s, 3H, o-methyl), 2.569 (s, 3H, c-methyl). ^{13}C NMR (150 MHz, d_6-DMSO): δ 188.2, 150.6, 148.5, 145.6, 145.0, 139.1, 130.6, 123.6, 123.3, 121.5, 113.5, 109.5, 103.8, 103.7, 56.9, 12.3. Melting point: degrades to black substance ca. 160 °C. TLC (in 4:1 ethyl acetate:hexanes) R_f = 0.15. Elemental analysis calculated for $C_{18}H_{15}N_5O_2{\cdot}C_4H_8O_2$ (trace ethyl acetate): C, 64.72; H, 4.60; N, 20.74. Found: C, 65.11; H, 4.71; N, 20.39.

Library Compounds. Compounds **1**−**8** used for initial screening of methuosis-inducing activity (Figure 1) were obtained from Hit2Lead.com, a division of Chembridge Corp. The identification numbers of the compounds were as follows: **1**, 5224450; **2**, 5224466; **3**, 5312531; **4**, 7995005; **5**, 7916760; **6**, 6161388; **7**, 5267766; and **8**, 6155359. All compounds are certified by the vendor to be at least 90% pure with NMR confirmation of structure.

Cell Culture. U251 human glioblastoma cells were purchased from the DCT Tumor Repository (National Cancer Institute, Frederick, MD). MCF-7 mammary carcinoma cells were obtained from The American Type Culture Collection (Rockville, MD). TMZ-resistant

U251 cells (U251-TR) were derived in our laboratory as described previously.[10] MCF-7 cells selected for resistance to doxorubicin[56] were provided by Amadeo Parissenti, Northeastern Ontario Regional Cancer Centre. Normal human skin fibroblasts were derived from a skin biopsy as described previously.[57] Unless stated otherwise, cell lines were maintained in Dulbecco's modified Eagle's medium (DMEM) with 10% (v/v) fetal bovine serum (FBS) (JR Scientific, Woodland, CA) at 37 °C in an atmosphere of 5% CO_2/95% air. Normal prestasis HMEC (specimen 184) were provided by Martha Stampfer, Lawrence Berkeley Lab (Berkeley, CA). The HMECs were maintained in M87A medium supplemented with cholera toxin and oxytocin, essentially as described.[58]

Cell Proliferation and Morphology. To generate cell growth curves, U251 cells were plated in 35 mm dishes (100000 cells/dish) and allowed to attach for 24 h. Thereafter, cells were treated with the indicated compounds dissolved in DMSO or with vehicle alone. At daily intervals, three parallel cultures were harvested from each group by trypsinization, and aliquots of cell suspension were counted in a Coulter Z1 particle counter. Phase-contrast images of live cells were obtained using an Olympus IX70 inverted microscope equipped with a digital camera and SPOT imaging software (Diagnostic Instruments, Inc., Sterling Heights, MI).

Cell Viability. Cells were seeded in 96-well plates, with four replicate wells for each culture condition. After addition of the indicated concentrations of compounds, cell viability was determined at a 48 h end point using a MTT-based assay as described.[10] Absorbance at 570 nm was quantified on a SpectraMax Plus 384 plate reader (Molecular Devices, Sunnyvale, CA).

Colony Formation. Cells were plated in 100 mm dishes at 2500 (U251 and U251-TR) or 1500 (MCF-7 and MCF-7 DoxR) cells per dish. Beginning on the day after plating, the cells were exposed to the indicated compounds for the periods of time noted in the figure legends. The medium was then replaced (without compounds), and cells were incubated for 10 days, with fresh medium added every 2 days. Colonies were visualized by washing with phosphate-buffered normal saline, fixing for 10 min with ice-cold 100% methanol, and staining with 1% (w/v) crystal violet (Acros Organics, Fisher Scientific, Pittsburgh, PA) in 35% methanol. After 2–3 washes with water, colonies containing at least 50 cells were counted using a dissecting microscope or a Protocol 2 colony counter (Synbiosis, Frederick, MD).

■ ASSOCIATED CONTENT

Ⓢ Supporting Information

Spectral data for all synthesized compounds. This material is available free of charge via the Internet at http://pubs.acs.org.

■ AUTHOR INFORMATION

Corresponding Author

*Tel: 419-530-2167. Fax: 419-530-1994. E-mail: paul.erhardt@utoledo.edu (P.W.E.). Tel: 419-383-4161. Fax: 419-383-6228. E-mail: william.maltese@utoledo.edu (W.A.M.).

Notes

The authors declare no competing financial interest.

■ ACKNOWLEDGMENTS

The work was supported by Grant R01 CA115495 (W.A.M.) from the National Institutes of Health.

■ ABBREVIATIONS USED

DBU, 1,8-diazabicyclo[5.4.0]undec-7-ene; DMF, dimethylformamide; DMSO, dimethylsulfoxide; GBM, glioblastoma multiforme; HMEC, human mammary epithelial cells; MTT, 3-(4,5-dimethylthiazol-2-yl)-2,5-diphenyl tetrazolium bromide; RT, room temperature; TMZ, Temozolomide

■ REFERENCES

(1) Stupp, R.; Mason, W. P.; van den Bent, M. J.; Weller, M.; Fisher, B.; Taphoorn, M. J.; Belanger, K.; Brandes, A. A.; Marosi, C.; Bogdahn, U.; Curschmann, J.; Janzer, R. C.; Ludwin, S. K.; Gorlia, T.; Allgeier, A.; Lacombe, D.; Cairncross, J. G.; Eisenhauer, E.; Mirimanoff, R. O. Radiotherapy plus concomitant and adjuvant Temozolomide for glioblastoma. *N. Engl. J. Med.* **2005**, *352*, 987–996.

(2) Norbury, C. J.; Zhivotovsky, B. DNA damage-induced apoptosis. *Oncogene* **2004**, *23*, 2797–2808.

(3) Ishii, N.; Maier, D.; Merlo, A.; Tada, M.; Sawamura, Y.; Diserens, A.-C.; Van Meir, E. G. Frequnt co-alterations of TP53, p16/CDKN2A, p14arf, PTEN tumor suppressor genes in human glioma cell lines. *Brain Pathol.* **1999**, *9*, 469–479.

(4) Furnari, F. B.; Fenton, T.; Bachoo, R. M.; Mukasa, A.; Stommel, J. M.; Stegh, A.; Hahn, W. C.; Ligon, K. L.; Louis, D. N.; Brennan, C.; Chin, L.; DePinho, R. A.; Cavenee, W. K. Malignant astrocytic glioma: Genetics, biology, and paths to treatment. *Genes Dev.* **2007**, *21*, 2683–2710.

(5) Bocangel, D. B.; Finkelstein, S.; Schold, S. C.; Bhakat, K. K.; Mitra, S.; Kokkinakis, D. M. Multifaceted resistance of gliomas to Temozolomide. *Clin. Cancer Res.* **2002**, *8*, 2725–2734.

(6) Overmeyer, J. H.; Kaul, A.; Johnson, E. E.; Maltese, W. A. Active ras triggers death in glioblastoma cells through hyperstimulation of macropinocytosis. *Mol. Cancer Res* **2008**, *6*, 965–977.

(7) Bhanot, H.; Young, A. M.; Overmeyer, J. H.; Maltese, W. A. Induction of non-apoptotic cell death by activated Ras requires inverse regulation of Rac1 and Arf6. *Mol. Cancer Res.* **2010**, *8*, 1358–1374.

(8) Swanson, J. A.; Watts, C. Macropinocytosis. *Trends Cell Biol.* **1995**, *5*, 424–428.

(9) Donaldson, J. G.; Porat-Shliom, N.; Cohen, L. A. Clathrin-independent endocytosis: A unique platform for cell signaling and PM remodeling. *Cell Signalling* **2009**, *21*, 1–6.

(10) Overmeyer, J. H.; Young, A. M.; Bhanot, H.; Maltese, W. A. A Chalcone-Related Small Molecule That Induces Methuosis, a Novel Form of Non-Apoptotic Cell Death, in Glioblastoma Cells. *Mol. Cancer* **2011**, *10*, 69.

(11) Cerny, J.; Feng, Y.; Yu, A.; Miyake, K.; Borgonovo, B.; Klumperman, J.; Meldolesi, J.; McNeil, P. L.; Kirchhausen, T. The small chemical vacuolin-1 inhibits Ca(2+)-dependent lysosomal exocytosis but not cell resealing. *EMBO Rep.* **2004**, *5*, 883–888.

(12) Go, M. L.; Wu, X.; Liu, X. L. Chalcones: An update on cytotoxic and chemoprotective properties. *Curr. Med. Chem.* **2005**, *12*, 481–499.

(13) Kamal, A.; Ramakrishna, G.; Raju, P.; Viswanath, A.; Ramaiah, M. J.; Balakishan, G.; Pal-Bhadra, M. Synthesis and anti-cancer activity of chalcone linked imidazolones. *Bioorg. Med. Chem. Lett.* **2010**, *20*, 4865–4869.

(14) Kumar, D.; Kumar, N. M.; Akamatsu, K.; Kusaka, E.; Harada, H.; Ito, T. Synthesis and biological evaluation of indolyl chalcones as antitumor agents. *Bioorg. Med. Chem. Lett.* **2010**, *20*, 3916–3919.

(15) Lindwall, H. G.; Order, R. B. V. 3-Indole aldehyde and certain of its condensation products. *J. Org. Chem.* **1945**, *10*, 128–133.

(16) Pasquini, S.; Mugnaini, C.; Brizzi, A.; Ligresti, A.; Di, M., V; Ghiron, C.; Corelli, F. Rapid combinatorial access to a library of 1,5-disubstituted-3-indole-N-alkylacetamides as CB2 receptor ligands. *J. Comb. Chem.* **2009**, *11*, 795–798.

(17) Lomenick, B.; Olsen, R. W.; Huang, J. Identification of direct protein targets of small molecules. *ACS Chem. Biol.* **2011**, *6*, 34–46.

(18) Hatanaka, Y.; Sadakane, Y. Photoaffinity labeling in drug discovery and developments: chemical gateway for entering proteomic frontier. *Curr. Top. Med. Chem.* **2002**, *2*, 271–288.

(19) Galardy, R. E.; Craig, L. C.; Printz, M. P. Benzophenone triplet: A new photochemical probe of biological ligand-receptor interactions. *Nat. New Biol.* **1973**, *242*, 127–128.

(20) Liu, D.; O'Leary, B.; Iruthayanathan, M.; Love-Homan, L.; Perez-Hernandez, N.; Olivo, H. F.; Dillon, J. S. Evaluation of a novel photoactive and biotinylated dehydroepiandrosterone analog. *Mol. Cell. Endocrinol.* **2010**, *328*, 56–62.

(21) Hasegawa, M.; Miura, T.; Kuzuya, K.; Inoue, A.; Won, K. S.; Horinouchi, S.; Yoshida, T.; Kunoh, T.; Koseki, K.; Mino, K.; Sasaki,

R.; Yoshida, M.; Mizukami, T. Identification of SAP155 as the target of GEX1A (Herboxidiene), an antitumor natural product. *ACS Chem. Biol.* **2011**, *6*, 229−233.
(22) Demopoulos, V. J.; Nicolaou, I. Electrophilic substitution of indole on the benzene moiety: A synthesis of 5-acyl- and 5-aroylindoles. *Synthesis* **1998**, *1998*, 1519−1522.
(23) Miller, D. K.; Gillard, J. W.; Vickers, P. J.; Sadowski, S.; Leveille, C.; Mancini, J. A.; Charleson, P.; Dixon, R. A.; Ford-Hutchinson, A. W.; Fortin, R. Identification and isolation of a membrane protein necessary for leukotriene production. *Nature* **1990**, *343*, 278−281.
(24) Palnitkar, S. S.; Bin, B.; Jimenez, L. S.; Morimoto, H.; Williams, P. G.; Paul-Pletzer, K.; Parness, J. [3H]Azidodantrolene: Synthesis and use in identification of a putative skeletal muscle dantrolene binding site in sarcoplasmic reticulum. *J. Med. Chem.* **1999**, *42*, 1872−1880.
(25) He, G.; Luo, W.; Li, P.; Remmers, C.; Netzer, W. J.; Hendrick, J.; Bettayeb, K.; Flajolet, M.; Gorelick, F.; Wennogle, L. P.; Greengard, P. Gamma-secretase activating protein is a therapeutic target for Alzheimer's disease. *Nature* **2010**, *467*, 95−98.
(26) Noland, W. E.; Smith, L. R.; Johnson, D. C. Nitration of indoles: II.The mononitration of methylindoles. *J. Org. Chem.* **1963**, *28*, 2262−2266.
(27) Melhado, L. L.; Leonard, N. J. An efficient synthesis of azidoindoles and azidotryptophans. *J. Org. Chem.* **1983**, *48*, 5130−5133.
(28) Uetrecht, J. Idiosyncratic drug reactions: current understanding. *Annu. Rev. Pharmacol. Toxicol.* **2007**, *47*, 513−539.
(29) Raja, S. M.; Clubb, R. J.; Ortega-Cava, C.; Williams, S. H.; Bailey, T. A.; Duan, L.; Zhao, X.; Reddi, A. L.; Nyong, A. M.; Natarajan, A.; Band, V.; Band, H. Anticancer activity of Celastrol in combination with ErbB2-targeted therapeutics for treatment of ErbB2-overexpressing breast cancers. *Cancer Biol. Ther.* **2011**, *11*, 263−276.
(30) Macpherson, L. J.; Dubin, A. E.; Evans, M. J.; Marr, F.; Schultz, P. G.; Cravatt, B. F.; Patapoutian, A. Noxious compounds activate TRPA1 ion channels through covalent modification of cysteines. *Nature* **2007**, *445*, 541−545.
(31) Yamakoshi, H.; Kanoh, N.; Kudo, C.; Sato, A.; Ueda, K.; Muroi, M.; Kon, S.; Satake, M.; Ohori, H.; Ishioka, C.; Oshima, Y.; Osada, H.; Chiba, N.; Shibata, H.; Iwabuchi, Y. KSRP/FUBP2 is a binding protein of GO-YO86, a cytotoxic curcumin analogue. *ACS Med. Chem. Lett.* **2010**, *1*, 273−276.
(32) Maresso, A. W.; Wu, R.; Kern, J. W.; Zhang, R.; Janik, D.; Missiakas, D. M.; Duban, M. E.; Joachimiak, A.; Schneewind, O. Activation of inhibitors by sortase triggers irreversible modification of the active site. *J. Biol. Chem.* **2007**, *282*, 23129−23139.
(33) Singh, J.; Petter, R. C.; Baillie, T. A.; Whitty, A. The resurgence of covalent drugs. *Nat. Rev. Drug Discovery* **2011**, *10*, 307−317.
(34) Stoll, R.; Renner, C.; Hansen, S.; Palme, S.; Klein, C.; Belling, A.; Zeslawski, W.; Kamionka, M.; Rehm, T.; Muhlhahn, P.; Schumacher, R.; Hesse, F.; Kaluza, B.; Voelter, W.; Engh, R. A.; Holak, T. A. Chalcone derivatives antagonize interactions between the human oncoprotein MDM2 and p53. *Biochemistry* **2001**, *40*, 336−344.
(35) Bois, F.; Boumendjel, A.; Mariotte, A. M.; Conseil, G.; Di Petro, A. Synthesis and biological activity of 4-alkoxy chalcones: potential hydrophobic modulators of P-glycoprotein-mediated multidrug resistance. *Bioorg. Med. Chem.* **1999**, *7*, 2691−2695.
(36) Hadjeri, M.; Barbier, M.; Ronot, X.; Mariotte, A. M.; Boumendjel, A.; Boutonnat, J. Modulation of P-glycoprotein-mediated multidrug resistance by flavonoid derivatives and analogues. *J. Med. Chem.* **2003**, *46*, 2125−2131.
(37) Liu, X. L.; Tee, H. W.; Go, M. L. Functionalized chalcones as selective inhibitors of P-glycoprotein and breast cancer resistance protein. *Bioorg. Med. Chem.* **2008**, *16*, 171−180.
(38) Edwards, M. L.; Stemerick, D. M.; Sunkara, P. S. Chalcones: A new class of antimitotic agents. *J. Med. Chem.* **1990**, *33*, 1948−1954.
(39) Dupeyre, G.; Chabot, G. G.; Thoret, S.; Cachet, X.; Seguin, J.; Guenard, D.; Tillequin, F.; Scherman, D.; Koch, M.; Michel, S. Synthesis and biological evaluation of (3,4,5-trimethoxyphenyl)indol-3-ylmethane derivatives as potential antivascular agents. *Bioorg. Med. Chem.* **2006**, *14*, 4410−4426.
(40) Boumendjel, A.; McLeer-Florin, A.; Champelovier, P.; Allegro, D.; Muhammad, D.; Souard, F.; Derouazi, M.; Peyrot, V.; Toussaint, B.; Boutonnat, J. A novel chalcone derivative which acts as a microtubule depolymerising agent and an inhibitor of P-gp and BCRP in in-vitro and in-vivo glioblastoma models. *BMC Cancer* **2009**, *9*, 242.
(41) Boumendjel, A.; Ronot, X.; Boutonnat, J. Chalcones derivatives acting as cell cycle blockers: potential anti cancer drugs? *Curr. Drug Targets* **2009**, *10*, 363−371.
(42) Ducki, S. Antimitotic chalcones and related compounds as inhibitors of tubulin assembly. *Anticancer Agents Med. Chem.* **2009**, *9*, 336−347.
(43) Champelovier, P.; Mininno, M.; Duchamp, E.; Nicolle, E.; Curri, V.; Boumendjel, A.; Boutonnat, J. Cytotoxicity of chalcone derivatives towards glioblastoma. *Anticancer Res.* **2011**, *31*, 3213−3218.
(44) Chao, T. C.; Chu, Z.; Tseng, L. M.; Chiou, T. J.; Hsieh, R. K.; Wang, W. S.; Yen, C. C.; Yang, M. H.; Hsiao, L. T.; Liu, J. H.; Chen, P. M. Paclitaxel in a novel formulation containing less Cremophor EL as first-line therapy for advanced breast cancer: A phase II trial. *Invest. New Drugs* **2005**, *23*, 171−177.
(45) McCarron, P. A.; Marouf, W. M.; Quinn, D. J.; Fay, F.; Burden, R. E.; Olwill, S. A.; Scott, C. J. Antibody targeting of camptothecin-loaded PLGA nanoparticles to tumor cells. *Bioconjugate Chem.* **2008**, *19*, 1561−1569.
(46) Danhier, F.; Lecouturier, N.; Vroman, B.; Jerome, C.; Marchand-Brynaert, J.; Feron, O.; Preat, V. Paclitaxel-loaded PEGylated PLGA-based nanoparticles: in vitro and in vivo evaluation. *J. Controlled Release* **2009**, *133*, 11−17.
(47) Emerson, D. L. Liposomal delivery of camptothecins. *Pharm. Sci. Technol. Today* **2000**, *3*, 205−209.
(48) Yang, T.; Cui, F. D.; Choi, M. K.; Lin, H.; Chung, S. J.; Shim, C. K.; Kim, D. D. Liposome formulation of paclitaxel with enhanced solubility and stability. *Drug Delivery* **2007**, *14*, 301−308.
(49) Park, Y. S. Tumor-directed targeting of liposomes. *Biosci. Rep.* **2002**, *22*, 267−281.
(50) Ruoslahti, E.; Bhatia, S. N.; Sailor, M. J. Targeting of drugs and nanoparticles to tumors. *J. Cell Biol.* **2010**, *188*, 759−768.
(51) Dolby, L. J.; Rodia, R. M. The periodate oxidation of heterocycles: II. 2-Methylindole and 2,3-diphenylindole. *J. Org. Chem.* **1970**, *35*, 1493−1496.
(52) Note that although no published analytical data were found, the following compounds have CAS numbers: compound **2**, 373618-91-8; compound **10**, 1237055-51-4; 2012.
(53) Tsukerman, S. V.; Nikitchenko, V. M.; Bugai, A. I.; Lavrishin, V. F. Synthesis of analogs of chalcones and derivatives of delta 2-pyrazoline based on 3-formylindole. *Khimiia Geterotsiklicheskikh Soedinenii* **1969**, *2*, 268−272.
(54) Gillard, J. W.; Belanger, P. Metabolic synthesis of arylacetic acid antiinflammatory drugs from arylhexenoic acids. 2. Indomethacin. *J. Med. Chem.* **1987**, *30*, 2051−2058.
(55) Beer, R. J. S.; Clarke, K.; Davenport, H. F.; Robertson, A. The chemistry of the melanins. III/. The synthesis of hydroxyindoles from p-benzoquinones. *J. Chem. Soc.* **1951**, 2029−2032.
(56) Guo, B.; Hembruff, S. L.; Villeneuve, D. J.; Kirwan, A. F.; Parissenti, A. M. Potent killing of paclitaxel- and doxorubicin-resistant breast cancer cells by calphostin C accompanied by cytoplasmic vacuolization. *Breast Cancer Res Treat.* **2003**, *82*, 125−141.
(57) Maltese, W. A.; De Vivo, D. C. Cholesterol and phospholipids in cultured skin fibroblasts from patients with dystonia. *Ann. Neurol.* **1984**, *16*, 250−252.
(58) Garbe, J. C.; Bhattacharya, S.; Merchant, B.; Bassett, E.; Swisshelm, K.; Feiler, H. S.; Wyrobek, A. J.; Stampfer, M. R. Molecular distinctions between stasis and telomere attrition senescence barriers shown by long-term culture of normal human mammary epithelial cells. *Cancer Res.* **2009**, *69*, 7557−7568.